



Cite this: *Mater. Adv.*, 2022, 3, 4402

## Electrospun curcumin-loaded polymer nanofibers: solution recipes, process parameters, properties, and biological activities

Petr Snetkov, \* Svetlana Morozkina, Roman Olekhnovich and Mayya Uspenskaya

Nanofibers loaded with biologically active compounds have attracted attention in recent years due to the controlled properties and targeted action. Curcumin, being the known regulator of many signaling pathways, and demonstrating many types of biological activities, most of them due to its antioxidant and anti-inflammatory effects, has attracted great attention for its increasing biological effects. In this review all known data about the electrospun curcumin-loaded fibers based on a polymer matrix have been collected and analyzed. In addition to the consideration of solution formulations and technological parameter dependencies, the curcumin release and biological effects of drug delivery systems are considered in detail.

Received 21st April 2022,  
Accepted 21st April 2022

DOI: 10.1039/d2ma00440b

rsc.li/materials-advances

### 1. Introduction

Electrospinning is known as an effective and topical method of fiber formation from polymer solutions (or melts) and allows obtaining nanofibrous materials with controlled properties for use in various applications, from air/water filtration and solar energy to tissue engineering and biomedicine. An example of polymer nanofibers is demonstrated in Fig. 1. Loading the pharmaceutically active substances and biologically active agents, having in general hydrophobic nature, enhances the solubility of the latter, and could lead to the reduction of effective dosage and decrease in side effects.

The natural polyphenol curcumin (1,7-bis(4-hydroxy-3-methoxyphenyl)-1,6-heptadiene-3,5-dione), also called diferuloylmethane, is a well-known regulator of many signaling pathways and demonstrates many types of biological activities, most of them due to its antioxidant and anti-inflammatory effects<sup>2,3</sup> and metabolic syndromes.<sup>4</sup> Its benefit for kidneys<sup>5</sup> has also been demonstrated.

However, curcumin has low solubility in water and as a result poor bioavailability, that results in poor absorption, rapid metabolism, and rapid elimination.<sup>6</sup>

Because the effectiveness of curcumin was also confirmed in clinical trials, including the treatment of gynecological diseases including pelvic inflammatory disease endometritis,<sup>7-9</sup> various delivery systems have been developed to overcome the restrictions for its clinical use.

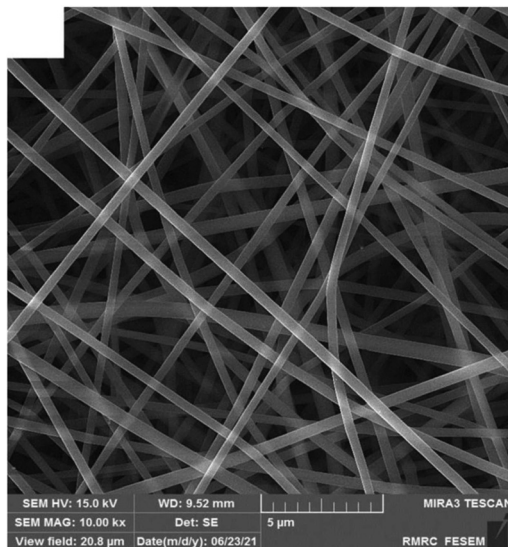


Fig. 1 An example of chitosan-gum Arabic nanofibers. Reproduced from ref. 1 with permission from Elsevier, 2022.

In this review we collected and divided all known curcumin-loaded polymer based fibers into groups depending on the polymer nature.

### 2. Electrospinning summary

Electrospinning (electrohydrodynamic jetting) is a highly effective, accessible, variable method for nanofiber fabrication



without sophisticated equipment from polymer solutions or melts, based on the exposure of high voltage on the polymeric spinning solution. Action of similar charges into the solution results in jet splitting with following nanofiber formation.<sup>10,11</sup>

The initial electrospinning technique requires a single needle (die, nozzle) for fabrication of monolithic polymer nanofibers from individual polymers or polymer blends. Core–shell nanofibers could also be obtained by the co-axial electrospinning method. The difference consists of the spinneret: there are two needles with different diameters placed coaxially into each other. Each needle is connected to an independent polymer solution feed line.<sup>11,12</sup> This method allows the fabrication of nanofibers consisting of various polymers, including polymers with different nature and hydrophobicity. It is an effective and topical technique to regulate drug release rate from polymer nanofibers, which is a challenging and advanced issue for modern drug delivery systems.

Apart from the usual co-axial electrospinning, it is known to design modified co-axial electrospinning, where a concentric spinneret with a slightly outstanding inner needle is used.<sup>12,13</sup> Such a modified spinneret improves the electrospinnability of the polymer solution, and prevents the mutual diffusion,

resulting in successful fabrication of smooth core–sheath nanofibers.

The next variation of electrospinning is the tri-axial technique. In this case, for the smooth fabrication of core–shell nanofibers the unspinnable solvent is used as an external technological agent.<sup>14</sup>

Schematic representations of the mono-axial, co-axial, and tri-axial electrospinning are demonstrated in Fig. 2.

Side-by-side electrospinning is also available.<sup>15</sup> In this method the polymer solutions are fed through the spliced spinneret, that allows for obtaining nanofibers stuck together along the long side. Such nanofibers are also named Janus electrospun nanofibers.<sup>16</sup>

The electrospinning process could be even more complicated to, for instance, quad-axial techniques, various treatments of the nanofibers following the electrospinning process, multi-layer collection of nanofibers (sandwich structure), etc.<sup>17</sup>

Note that apart from the linear nanofibers, the beads-on-a-string structures<sup>18</sup> and mixture of nanofibers and nanoparticles<sup>19</sup> were also obtained, which opens new scientific directions and allows the fabrication of modern polymeric materials with unique properties.



Petr Snetkov

*Dr Petr Snetkov currently holds the Senior Engineer position at Center of Chemical Engineering, ITMO University. He graduated with honors from Saint-Petersburg State University of Film and Television, Faculty of Photography and Technology of Recording Materials, in 2012 as an Engineer in Technology of motion picture-photographic materials and magnetic storage media (five-year full-time program). From 2012 until now Petr Snetkov has worked*

*in the field of development, research, and production of polymeric and elastomeric materials and composites for various industrial fields. His postgraduate education started in 2017 at ITMO University in the field of Technology and processing of polymers and composites. He graduated from ITMO University as a Researcher, High-Researcher doctorem (in Chemical Technologies), in 2021 with following successful PhD defence with the thesis entitled "Fabrication of hyaluronic acid-based fibrous materials by electrospinning technique". He is an author of 10+ international scientific publications, 20+ national scientific articles, one Russian invention, and one study guide. Petr Snetkov is involved in several grants from the Russian Foundation for Basic Research, the Ministry of Science and Higher Education of the Russian Federation, and the Russian Science Foundation. His main scientific research areas are as follows: biocompatible materials, biodegradation, biologically active agents, drug delivery systems, electrospinning, hyaluronic acid, nanofiber technology, nanofibers, polymer chemistry, polymeric nano- and microparticles, polymeric nanocomposites, etc.*



Svetlana Morozkina

*Dr Svetlana Morozkina currently holds the position of Assoc. Prof. at the ITMO University. She graduated from Saint-Petersburg State University in 1997 and got PhD degree in 2001. After Post-Doc position (2001–2004) she organized a research group in the field of steroid estrogens in 2004 at the Department of Natural Products Chemistry at Saint-Petersburg State University. She has broad collaborations: Imperial College of London,*

*DKFZ, Charite Klinikum, Erlangen University, University of Lausanne, Biomedicum Centre of Helsinki University, Merck Company, and Bayer Schering Pharma. She was/is a member of Organizing Committees of International Conferences; the expert of European Commission ERA.Net RUS Pilot Joint Call in Innovation Projects; an invited lecturer (University of Jyvaskyla and KU Leuven); and a member of the jury of the Intel Baltic Science and Engineering Fair. Since September 2017 she continues research at ITMO University in the fields of drug development, medicinal chemistry, bioorganic chemistry, natural products and drug delivery systems. She is the author of 60+ publications and 26 patents.*



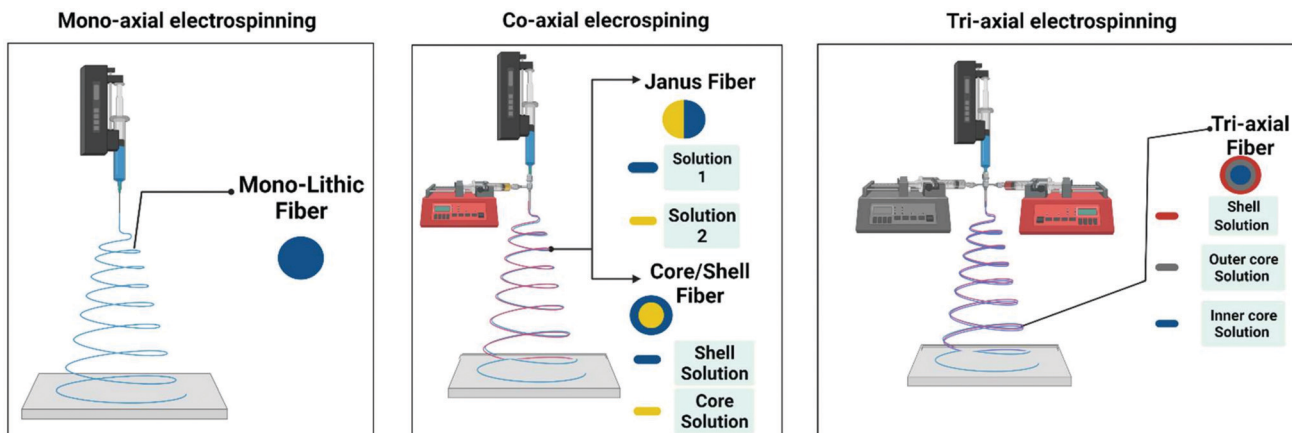


Fig. 2 Schematic representations of the mono-axial, co-axial, and tri-axial electrospinning techniques. Reproduced from ref. 10, with permission from MDPI, 2022.

### 3. Polymers used for curcumin-loaded fiber formation

A variety of polymers are widely used to obtain nanofibers by the electrospinning technique. Polymers are usually divided into synthetic (polycaprolactone, polyurethane, polylactic acid, copolymers of acrylic acid, polyvinyl alcohol, poly ethylene glycol, *etc.*) and natural (polysaccharides, such as alginate, chitosan, hyaluronic acid; and proteins, *e.g.*, gelatin, silk fibroin, zein corn, *etc.*). Natural polymers are preferable for bioengineering application due to their high biodegradability and biocompatibility; however, nanofibers based on such polymers are difficult to electrospin and in general have low mechanical properties.



Roman Olekhnovich

*Roman Olekhnovich is a Assoc. Prof. at the ITMO University. He defended his PhD degree in 2010. He is the author of 40+ publications. Currently his research interests focus on hydrogels for agriculture and wastewater treatment, polymeric nanocomposites, electrospun nanofibers, and biochemical sensors.*

This review covers the widely used polymers which are most suitable as a carrier for curcumin delivery in the form of fibers.

#### 3.1 Poly( $\epsilon$ -caprolactone) and polydioxanone

Poly( $\epsilon$ -caprolactone) (PCL) is a biocompatible, biodegradable, semi-crystalline, hydrophobic biopolymer, which could be used as a drug delivery system with prolonged action due to its slow degradation. It is graded according to the molecular weight (Mn). PCL can be mixed with other polymers/biopolymers to improve the physical, physico-chemical, and exploitative characteristics of the resulting composition and for the regulation of drug release rate.<sup>20</sup>

Jonathan G. Merrel *et al.*<sup>21</sup> used PCL dissolved in a chloroform:methanol solvent mixture (3:1, v/v) for the



Mayya Uspenskaya

*Prof. M. Uspenskaya graduated from the Department of Macromolecular Compounds at Saint-Petersburg State University (Russia) in 1994. She defended her PhD degree in 2010. Her current position is a full Professor, Director of Chemical Engineering Center at ITMO University. She is the author of 100+ publications and 10 patents. She was a supervisor of 50+ magisters and 10+ PhDs. Under her supervision many*

*research grants as well from government sources as applied researches for commercial firms were realized in the field of hydrogel materials and sensors, and drug delivery systems. Currently Prof. M. Uspenskaya's research interests focus on radical polymerization, super-water absorbents, hydrogels, cross-linked chain polymers, polymeric nanocomposites, delivery of the medical products, biochemical sensors and diagnostic tools.*



electrospinning of blank or curcumin-loaded nanofibers. The authors demonstrated that the optimal PCL concentration is equal to 15% (w/v) which allows for obtaining bead-free nanofibers with the diameters in the range of 300–400 nm. Interestingly, the addition of curcumin (3% w/w to PCL) could result in the widening of the nanofiber diameter distribution to 200–800 nm. The further increase of curcumin content to 17% w/w did not lead to a significant change in the fiber morphology. Curcumin release rate (*in vitro*) could be characterized as time-delayed: approximately 35 µg and 20 µg curcumin by Day 3 from curcumin-loaded fibers with 17% w/w and 3% w/w, respectively. Anti-oxidant properties of the curcumin-loaded nanofibers were confirmed by oxygen radical absorbance capacity (ORAC). The authors also demonstrated the high level of cytocompatibility, cytoprotective effectiveness, and anti-inflammatory activity of curcumin-loaded nanofibers and their ability to accelerate the healing process *in vivo* (diabetic mouse model).

Gang Guo *et al.*<sup>22</sup> successfully obtained pure and curcumin-loaded nanofibers based on a poly(3-caprolactone)-poly(ethylene glycol)-poly(3-caprolactone) copolymer (PCEC) dissolved in dichloromethane/isopropanol (4:1 v/v). The curcumin was added directly into the polymer solution in the amounts from 5 to 20 wt% in the ratio to PCEC. The study demonstrates that curcumin concentration from 5 to 20 wt% did not lead to a significant variation of the fiber morphology and diameter distribution. At the same time an increase of curcumin content has a distinct effect on the *in vitro* drug release profile. For instance, by day 14 the maximum curcumin amount was equal to 54.8%, 73.5%, 88.5%, and 90.7% for PCEC fibers with 5, 10, 15, and 20 wt% of curcumin, respectively. The *in vitro* cytotoxicity of curcumin-loaded nanofibers demonstrated high effectiveness against the rat glioma 9L cells in comparison with pure PCEC nanofibers. Moreover, anticancer activity of the curcumin-loaded nanofibers against the glioma 9L cells was observed over the whole period of cytotoxicity assay (72 h), while the potency of native curcumin was lost within 48 h.

By contrast, Shao-Zhi Fu *et al.*<sup>23</sup> used another solution technique. PCEC was initially dissolved in dichloromethane followed by mixing with curcumin solutions in ethanol. The curcumin contents were equal to 5, 10, 15, and 20 wt% in the ratio to PCEC. It was found that the blank nanofibers were relatively smoother and had a larger diameter. With the curcumin addition the fiber agglutination was observed. Moreover, individual and associated toroid structures were found in the fibrous material. Curcumin was successfully loaded into PCEC matrixes and no curcumin crystals were found on the fiber surface. There was slow curcumin release rate from the loaded nanofibers: 52.7%, 66.4%, 78.5%, and 87.2% for the nanofibers with 5%, 10%, 15%, and 20% curcumin, respectively. The developed curcumin-loaded PCEC nanofibers possess high absorbing capacity of free radicals and low cytotoxicity against the primary mouse dermal fibroblast cell culture. Note that curcumin-loaded nanofibers accelerate the wound healing process (full-thickness skin defect model) in comparison with the control group and pure PCEC group (Fig. 3), which have high-potential for application in wound repair.

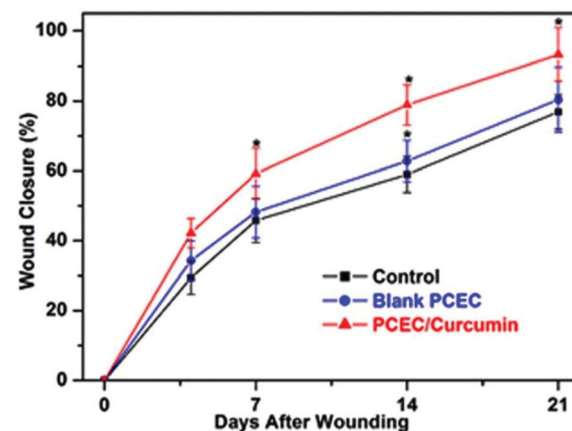


Fig. 3 Time dependence of percent wound healing of the full-thickness skin defect model in Wistar rats. Reproduced from ref. 23, with permission from John Wiley and Sons, 2022.

Marziyeh Ranjbar-Mohammadi with co-authors<sup>24</sup> fabricated curcumin-loaded membranes based on PCL and PCL with gum tragacanth (GT). In the latter case polymer solutions were separately prepared with further mixing in 1:2 GT/PCL mass ratio. An increase of curcumin concentration leads to the increase of PCL fiber diameter, narrowing the diameter distribution, and to the increase of polymer solution viscosity. By contrast, the loading of curcumin into a PCL/GT matrix did not have a significant effect on nanofiber diameter, but had influence on morphology. Although GT was added for decreasing the hydrophobicity of PCL membranes, and eventually for an improvement of the biocompatibility and cell adhesion, curcumin demonstrated the higher influence on hydrophobicity decrease. Curcumin also helped to enhance the mechanical properties of nanofibers and their stability towards degradation. The nanofibers favoured cellular growth, cell attachment, and cell proliferation and could retain the initial cell morphology for 15 days. The curcumin release was without a burst effect.

Further investigations demonstrated the high antibacterial activity of curcumin-loaded PCL/GT nanofibers against methicillin resistant *Staphylococcus aureus* (99.9%) and extended spectrum  $\beta$ -lactamase (85.14%).<sup>25</sup> PCL/GT nanofibers containing curcumin could also accelerate the wound repair process. Moreover, the increase of collagen content during the treatment of diabetic wounds was stimulated by nanofibers, which could be a catalyst for the healing process in early stages. Blood glucose level decrease was also detected in the animal group treated with the nanofibers obtained in comparison with the control group.

The next study<sup>26</sup> describes curcumin-loaded nanofibers based on PCL, which could be used as a barrier to prevent adhesion formation. Note that a drum collector with a rotation rate equal to 300 rpm was used for the fiber fabrication from PCL chloroform/methanol (4:1 v/v) binary solutions with the different polymer concentrations. The increase of the fiber diameter with the polymer concentration increase was



detected. PCL concentration increase led to the formation of smooth fibers without beads. Curcumin-loaded PCL nanofibers could prevent the formation of postsurgical adhesion in the animal model for 50% compared to the control group. After 30 days the curcumin release from the nanofibers was equal to 30%.

Minh Son Hoang and co-authors<sup>27</sup> successfully obtained curcumin-loaded polycaprolactone/chitosan (PCL/CTS) nanofibers which have a diameter range from 267 nm to 402 nm. The authors analyzed in detail the physical characteristics of PCL/CTS spinning polymer solutions, as well as the effect of the technological parameters on solution electrospinnability and fiber morphology. Curcumin was released from nanofibers within 100 h (nearly 80%); however, further release rate decreased and around 90% of curcumin was released after 650 h.

The authors of another study<sup>28</sup> gave the highest priority to solution characteristics, relative humidity, and its influence on nanofiber morphology and diameter distribution. Thus, a significant increase of the nanofiber average diameter from 100 nm to 145 nm was detected after the relative humidity level was changed from 40% to 60%, which confirms the sensitivity of hydrophobic polymer spinning systems to environment conditions. Note that nanofiber formation was achieved by the needleless electrospinning technique. The curcumin-loaded PCL nanofibers demonstrated optimal swelling behavior (254% after 48 h). Curcumin release ratio is slow and without any burst release behavior.

Y. Emre Bulbul *et al.*<sup>29</sup> successfully obtained the electrospun nanofibers based on a blend of PCL and polyethylene oxide (PEO). Apart from curcumin the authors added into spinning solutions the nanotubes based on the modified aluminosilicate clay mineral halloysite, which led to the maximization of curcumin encapsulation efficiency and resulted in slower curcumin release from the nanofibers. In addition, curcumin/halloysite nanotube-loaded PCL/PEO nanofibers demonstrated high level of toxicity against MCF-7 breast cancer cells.

A recent study<sup>30</sup> reported the curcumin-loaded nanofibers based on PCL, poly[(R)-3-hydroxybutyric acid] (PHB), and its blend (1:1 w/w). Addition of PHB into the polymer solution has an effect on the increase of the porosity of electrospun membranes (1.4-fold in comparison with pure PCL nanofibers). Moreover, it leads to the reduction of burst release of curcumin compared to the PCL membrane, resulting in the controllable curcumin release profile.

B. Caglayan and G. Basal<sup>31</sup> demonstrated a PCL/silk fibroin nanofibrous scaffold loaded with curcumin. Silk fibroin addition could decrease the hydrophobicity of PCL nanofibers, resulting in the improvement of the water capacity. In spite of the strength decrease, such nanofibers could be used in postoperative application. The release profile of curcumin had initial burst character within 3 h (87% of the loaded curcumin) with further stable and slow release for 10 days. Note that nanofibers based on silk fibroin are listed in the individual subsection.

The next study describes the effectiveness of electrospun curcumin-loaded PCL homogeneous nanofibers with diameters

ranging from 441 to 557 nm to support the formation of bacterial biofilm.<sup>32</sup> Interestingly, the authors used a solution preparation method different from the other studies: curcumin was preliminarily dissolved in ethanol with further addition into 10% PCL chloroform solution at various proportions (from 2.0 to 10.0% v/v). As a result, the nanofibers obtained allow the prevention of pathogenic biofilm formation caused by the three bacteria strains: *Pseudomonas aeruginosa*, *Staphylococcus aureus* and *Escherichia coli*.

Polydioxanone (PDO) is a biodegradable polymer generally applied for various biodegradable medical devices with varying shapes, sizes, and geometry due to its non-antigenic and non-pyrogenic nature and the minimal tissue reaction during the absorption and degradation after surgical intervention and device implantation.<sup>33</sup>

Pierre-Alexis Mouthuy *et al.*<sup>34</sup> prepared curcumin-loaded PDO nanofibers. Interestingly, the nanofibers containing low curcumin quantity had higher repairing capacity in comparison with the highly filled nanofibers. The results demonstrate that the application of PDO nanofibers with high curcumin concentration (1% and 10%) could lead to the inhibition of the normal human skin fibroblast proliferation or even apoptosis. This is explained by the curcumin concentration in the medium which was close to the toxicity level. By contrast, nanofibers with low curcumin concentrations could stimulate the metabolic activity and proliferation of the normal human dermal fibroblasts, which is more preferable for tissue repair and wound healing.

The results mentioned above suggest the high potential of nanofibers based on PCL with curcumin addition. Such materials could be applied in various biomedical and biotechnological areas, such as chemotherapy, wound healing, drug delivery systems, *etc.*

The summarized information about the solution recipes and technological parameters of electrospinning is listed in Table 1.

### 3.2 Polyurethanes

Polyurethanes (PU) belong to a special family of polymers with urethane (or carbamate) groups in the polymer chain. PU could be synthesized by the reaction of a polyol (polyester/polyether) and isocyanate (typically a diisocyanate) with chain extenders, polymerization accelerators or under UV-irradiation.<sup>35,36</sup> PU are widely used in various areas, including some specific biomedical applications, such as drug delivery systems, nanofibers, scaffolds, implants, antibacterial coatings, *etc.*<sup>37</sup> Obviously, the biological and degradation properties of materials based on PU mainly depend on polyol function within PU. Therefore, it is preferable to use biodegradable PCL, polyethylene glycol (PEG), polypropylene oxide (PPO), and similar polymers for the synthesis of PU.

Ali Shababdoust with coauthors described curcumin-loaded PU nanofibers electrospun from hexafluoroisopropanol (HFIP) solutions.<sup>38</sup> Note that a drum collector with 1000 rpm rotation was used. Two types of PCL for PU synthesis were used: with 2.0 kDa Mn and with 0.53 kDa Mn, hereinafter named PU2000 and PU530, respectively. The curcumin release behavior from PU nanofibers could be characterized as burst release within



**Table 1** Solution recipes and technological parameters of the electrospinning from the solutions based on poly( $\epsilon$ -caprolactone)

Polymer base ( $M_w$ , kDa)	$C_{PB}$ , w/v%	Solvent(s)	$C_{cur}$ , % w/w (v/v)	FR, mL h <sup>-1</sup>	$U$ , kV	$H$ , mm	$D_{fib}$ , nm	Ref.
PCL (65.0)	15.0	CHCl <sub>3</sub> : methanol (3 : 1, v/v)	0 3; 17	2.0	25.0	100	300–400 200–800	21
PCEC (61.8)	8.0	DCM : isopropanol (4 : 1, v/v)	0.0 5.0 10.0 15.0 20.0	3.0	18.0	120	~4200 ~2700 ~2300 ~3800 ~4500	22
PCEC (62.0)	6.0	DCM : EtOH (n.r.)	5; 10; 15; 20	6.0	18.0	120	up to ~4000	23
PCL (80.0)	20.0	Acetic acid (90% v/v)	0.0 1.0 3.0	1.0	15.0	150	288 $\pm$ 36 667 $\pm$ 33 836 $\pm$ 23	24
PCL (80.0)	20.0	Acetic acid (90% v/v)	0.0 3.0	1.0	15.0	150	164 $\pm$ 34	24
GT	7.0						191 $\pm$ 24	
PCL (80.0)	6.0	CHCl <sub>3</sub> : methanol (3 : 1, v/v)	6.0	0.7	22.0	100	220 $\pm$ 100 255 $\pm$ 100	26
	7.0						385 $\pm$ 150	
	8.0						585 $\pm$ 179	
PCL (70.0)	9.0	Acetic acid/acetone (3 : 1 v/v)	1.0–5.0	0.3	15.0	80	267–402	27
CTS (100.0–300.0)	1.0							
PCL (80.0)	3.0	DCM	0.1	—	45.0	210	62–1760	28
PCL (80.0)	18.0	DMF/CHCl <sub>3</sub> (10 : 90 v/v)	0.0	0.5	15	150	647 $\pm$ 106	29
PEO (100.0)	1.0							
PCL (80.0)	18.0	DMF/CHCl <sub>3</sub> (10 : 90 v/v)	5.0	1.4	17	200	2252 $\pm$ 736	29
PEO (100.0)	1.0							
PCL (80.0)	12.0	THF/DMF (1 : 1, v/v)	0.0 1.0 1.0	0.5	17.5	180	320 $\pm$ 20 340 $\pm$ 180	30
PHB (1000.0)	6.0	CHCl <sub>3</sub> /DMF (9 : 1, v/v)	0.0 1.0	3.0	20.0	280	3330 $\pm$ 20 3450 $\pm$ 850	30
PCL (80.0)	9.0	CHCl <sub>3</sub> /DMF (9 : 1, v/v)	1.0	2.0	20.0	180	520 $\pm$ 190	30
PHB (1000.0)	(Total)							
PCL (80.0)	10.0	Formic acid	0.0	2.0	15.0	150	105–441	31
	15.0		0.0	2.0	20.0	150	100–370	
PCL (80.0)	15.0	Formic acid	0.0	1.0–3.0	15.0–25.0	150	107–667	31
Silk fibroin	15.0		3.0				100–2320	
PCL (24.0)	10.0	CHCl <sub>3</sub>	0.0	1.0	20.0	100	500 $\pm$ 165 1734 $\pm$ 525	32
	2.0		2.0				709 $\pm$ 254	
	2.5		5.0				441 $\pm$ 154	
	5.0		10.0				557 $\pm$ 161	
PDO	9.0	HFIP	0.0 0.001 0.01 0.1 1.0 10.0	n.r.	6.0	200	1800 $\pm$ 700 1900 $\pm$ 600 1900 $\pm$ 900 2100 $\pm$ 900 1600 $\pm$ 600 1100 $\pm$ 600	34

$C_{cur}$  – curcumin concentration; CHCl<sub>3</sub> – chloroform; CTS – chitosan; DCM – dichloromethane;  $D_{fib}$  – average fiber diameter; DMF – *N,N*-dimethylformamide; EtOH – ethanol; FR – feed rate; GT – gum tragacanth;  $H$  – distance (height) between the spinneret and collecting electrode; HFIP – hexafluoroisopropanol; n.r. – not reported; PCL – poly( $\epsilon$ -caprolactone); PDO – polydioxanone; PHB – poly[(*R*)-3-hydroxybutyric acid], poly(3-hydroxybutyrate); THF – tetrahydrofuran;  $U$  – applied high voltage level.

24 h, with further stable release over 450 h. Antibacterial effectiveness against *Escherichia coli* *in vitro* was demonstrated with up to 97% activity.

The electrospun nanofibers with a diameter range of 400–900 nm based on a series of amphiphilic-block segmented PU were described.<sup>39</sup> Higher mechanical properties and hydrophilicity in comparison with polyurethane based on PCL were investigated.

The release profile of curcumin showed a stable rate within 18 days. The antibacterial effect of curcumin-loaded PU nanofibers was equal to 93% and 100% against *Staphylococcus aureus* and *Escherichia coli*, respectively. The nontoxic effect was also confirmed by metabolic activity of L929 mouse fibroblast cells.

Horzum Polat with coauthors<sup>40</sup> obtained electrospun nanofibers based on biobased PU Pearlthane<sup>®</sup> ECO D12T85. Special attention was given to an optimization of the electrospinning process by varying technological parameters (applied voltage, flow rate, and the distance between the spinneret and collector), as well as solution recipes. Thus, the PU and curcumin-loaded PU nanofibers with a diameter range of 250–850 nm and 525–960 nm, respectively, were demonstrated.

P. Sagitha *et al.*<sup>41</sup> provided an extensive study of PU pH-responsive bead-free nanofibers with a smooth surface and narrow fiber diameter. The authors used 10% Tecoflex EG85A and dextran dissolved in THF/DMF binary solvent. Dextran addition into (PU) nanofibers resulted in the rise of its



mechanical properties, hydrophilicity level, vapour permeability, and biodegradability. The proliferation of embryonic fibroblasts, their adhesion on PU nanofibers and viability were confirmed. Synergistic antibacterial effectiveness against *Staphylococcus aureus* was detected (Fig. 4).

The results show the possibility of the application of nanofibers based on PU for pH-controlled release carriers and wound dressing with antibacterial properties.

The summarized information about the solution recipes and technological parameters of the electrospinning is listed in Table 2.

### 3.3 Poly(lactic) acid and its derivatives

Poly(lactic) acid (PLA) being an aliphatic polyester plays a general role in the biomedical and bioengineering field for various applications: surgical sutures, clamping screws, targeted drug delivery systems, *etc.* The mechanism of PLA degradation *in situ* based on hydrolysis leads to elimination of the necessity of repeated surgeries to remove the medical device.<sup>42</sup>

Priscilla P. Luz with collaborators<sup>43</sup> described curcumin-loaded poly(lactic acid) (PLA) and poly(lactic-*co*-glycolic acid) (PLGA) electrospun nanofibers with an average diameter equal to 3600 nm and 123.6 nm, respectively. The first one could be characterized as nonrigid and with an irregular surface, while the second one was porous and had rigidity. The curcumin contents in the PLA and PLGA nanofibers were  $4.0 \pm 0.2\%$  and  $1.8 \pm 0.1\%$ , respectively.

Govindaraj Perumal *et al.*<sup>44</sup> obtained the blank and curcumin-loaded nanofibers based on poly DL lactic acid (PLDA) with the addition of hyperbranched polyglycerol (HPG), as this polymer has great potency in tissue engineering. After the addition of HPG into PDLA nanofibers the latter exhibit hydrophilic character, associated with the increase of hydroxyl group appropriated to HPG. The high cytocompatibility of nanofibers obtained with embryonic Swiss mouse fibroblast cells (3T3 line) was demonstrated.

The next study<sup>45</sup> demonstrates a biocompatible and biodegradable polymer membrane composed of cross-linked polyvinyl alcohol/polyethylene oxide film and curcumin-loaded PLA nanofibers. The prepared material had a high level of water absorption, vapor permeability, and excellent mechanical

properties. The burst release profile in the first release stage (60 min) was detected. At the second stage curcumin release could be characterized as constant, sustained, and slow.

K. Matskou *et al.*<sup>46</sup> obtained bead-free nanofibers from the mixture of PLA solution in DMF/DCM and chitosan solution in DMF/deionized water. Curcumin was dissolved in ethanol and added into the polymer solution before electrospinning. The addition of curcumin leads to the increase of the degradation percentage. Curcumin release profile was measured during 91 days and had three phases: burst release in the first 24 hours (first phase) and controlled and slow character in the second (84 days) and third phases (the latter 7 days). The cytocompatibility of nanofibers with murine fibroblast L929 was successfully confirmed. Moreover, good cell attachment and proliferation was proved.

The next paper<sup>47</sup> describes poly(L-lactic acid) nanofibers without and with contents of curcumin having an average diameter equal to 386 nm and 333–380 nm, respectively. Antioxidant activity, non-toxicity of nanofibers to human adult dermal fibroblasts (HDF), cell adhesion and proliferation were studied in detail. Antioxidant activity of the curcumin released from PLLA nanofibers after immersion (0.25–8.0 h) varies from 42.50% to 52.96%. The curcumin-loaded PLLA nanofibers demonstrated the better HDF attachment and proliferation in comparison with native PLLA nanofibers: the cell attachment and proliferation enhanced with drug content increase. HDF maintained their shape and exhibited a good adhesion and spreading on the native and curcumin-loaded nanofibers, as well as a control.

Leila Moradkhannejhad *et al.*<sup>48</sup> analyzed the effect of polyethylene glycol (PEG) concentration and its molecular weight on the curcumin release rate from electrospun PLA/PEG membranes. PEG has molecular weights equal to 0.40, 0.60, 1.50, 3.35, and 6.0 kDa. The first group of the solutions contained 10 wt% PLA and various concentrations of PEG (from 0.0 to 20.0 wt% at a pitch of 5.0 wt% with respect to PLA). The second group of solutions included 10 wt% PLA and 10 wt% PEG (related to PLA) with the different molecular weights. Curcumin release could be promoted as a result of PEG molecular weight decrease or PEG concentration increase (Fig. 5). There are also some differences in the degradation in PBS (weight loss, Fig. 6), which is a prerequisite for the development of advanced fibrous materials with the controllable biodegradable properties. Good cell attachment was confirmed in MG-63 cell adhesion assay.

Sara Rasouli *et al.*<sup>49</sup> obtained the curcumin- and chrysanthemic acid-co-loaded nanofibers based on PLGA/PEG copolymers and confirmed their significant potency to inhibit T47D breast cancer cells. Co-loaded nanofibers in comparison with single curcumin-loaded ones had an increased average diameter, improved physico-mechanical characteristics, and prolonged drug release profile under mimicked physiological condition (pH 7.4, 37 °C) for 7 days. Fig. 7 demonstrates the *in vitro* cytotoxicity of the drug-loaded membranes against the T47D breast cancer cells after 3 days of the incubation.

In summary, the above-mentioned studies confirmed the possibility for the application of PLA nanofibers with curcumin in transdermal and cancer drug delivery.

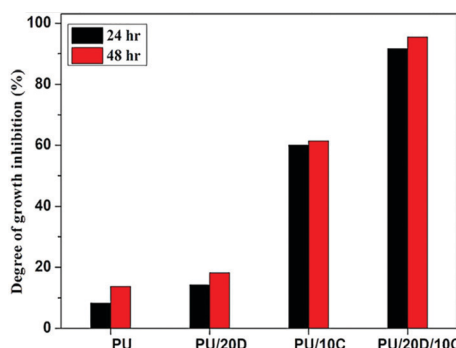


Fig. 4 Antibacterial activity of curcumin-loaded PU and PU/dextran nanofibers. Reproduced from ref. 41, with permission from Elsevier, 2022.



Table 2 Solution recipes and technological parameters of electrospinning from the solutions based on PU

Polymer base	$C_{PB}$ , w/v%	Solvent(s), w/w or v/v	$C_{cur}$ , % w/w	FR, mL h <sup>-1</sup>	U, kV	H, mm	$D_{fib}$ , nm	Ref.
PU2000	20.0	HFIP	0.0	0.5	20.0	210	$172 \pm 64$	38
			5.0				$256 \pm 110$	
			10.0				$247 \pm 107$	
PU530	30.0	HFIP	0.0	0.5	20.0	210	$200 \pm 80$	38
			5.0				$284 \pm 112$	
			10.0				$274 \pm 107$	
PCL-based polyurethane (PU)	20.0	HFIP	0.0	0.5	20.0	210	$172 \pm 64$	39
			5.0				$256 \pm 110$	
			10.0				$274 \pm 107$	
Di-block PEG-PCL-based polyurethane (PCE)	20.0	HFIP	0.0	0.5	20.0	210	$427 \pm 218$	39
			5.0				$546 \pm 279$	
			10.0				$651 \pm 209$	
Tri-block PEG-PCL-PEG-based polyurethane (PECE)	20.0	HFIP	0.0	0.5	20.0	210	$663 \pm 300$	39
			5.0				$805 \pm 170$	
			10.0				$889 \pm 227$	
Pearlthane <sup>®</sup> ECO D12T85	12.5	DMF	0.0	1.0	12.5	170	$480 \pm 150$	40
			1.0				$525 \pm 70$	
			5.0				$960 \pm 210$	
Taxoflex EG 85 A Dextran (70.0)	10.0 5.0–25.0	THF/DMF 6 : 4 v/v	10.0	1.0	15.0	170	$780 \pm 155$	41
							$\sim 401$	

$CHCl_3$  – chloroform;  $D_{fib}$  – average fiber diameter; EtOH – ethanol; GT – gum tragacanth; HFIP – hexafluoroisopropanol; PCE – di-block PEG-PCL-based polyurethane; PECE – tri-block PEG-PCL-PEG-based polyurethane; PHB – poly[(R)-3-hydroxybutyric acid], poly(3-hydroxybutyrate).

The information about the solution recipes and technological electrospinning parameters is listed in Table 3.

### 3.4 Polyvinylpyrrolidone

Polyvinylpyrrolidone (polyvidone, povidone, PVP) is a universal biodegradable, biocompatible, hydrophilic polymer, which is widely used in medicine, food, cosmetics, and bioengineering.<sup>50</sup> Moreover, good electrospinnability of PVP solutions was demonstrated recently.<sup>51</sup>

Annisa Rahma and collaborators fabricated PVP nanofibers with curcumin by the electrospinning technique.<sup>52</sup> The authors added a surfactant non-ionic polysorbate 20 (polyoxyethylene (20) sorbitan monolaurate) into the spinning solution and analyzed its effect on the fiber morphology and curcumin release rate. As a result, the addition of polysorbate 20 leads to the fiber diameter decrease and narrowing of the diameter distributions: from 540–660 nm (without surfactant) to 350–400 nm (with surfactant). By contrast, polysorbate 20 resulted in the increase of the curcumin release from the fibers, especially at the first stage. More than 50% of the curcumin was released regardless of spinning solution recipes.

The next study<sup>53</sup> demonstrates bead-free, uniform, and smooth curcumin-loaded PVP nanofibers, their dissolution profile, pharmacokinetics, bioavailability, and cytotoxicity (*in vitro* and *in vivo*) against the murine melanoma cell line B16. The optimal curcumin concentration is equal to 10 wt% (to PVP). A further increase of curcumin concentration led to curcumin crystallization on the fiber surface. Experiments confirmed that curcumin-loaded PVP fibers have high capacity to dissolve in PBS solutions: dissolution rate was equal to 90% for 15 min with the rate reduction to 89% at 48 h; however, the precipitation of curcumin was detected. In summary, the drug-loaded nanofibers exhibited increased bioavailability and

strong antitumour effectiveness. Photo of the tumours exposed to various compositions and the time-dependent behaviour of tumour volume are demonstrated in Fig. 8.

Apart from the native curcumin the derivatives could also be used as an effective drug component loaded into polymer nanofibers. Thus, Ravikumar Rrmaswamy *et al.*<sup>54</sup> developed PVP nanofibers containing tetrahydro curcumin (THC). The authors used a rotary drum collector (25 rpm) for spinning. Optimal formula of the spinning solution containing 10 wt% PVP and 10 wt% THC (in the ratio to the PVP) allows for obtaining bead-free nanofibers with a smooth and fine morphology, which was demonstrated by tetrahydro-curcumin release equal to 91% during the first 5 min. The authors declare the suitability of nanofibers formed for buccal delivery systems.

A recent study<sup>55</sup> demonstrates PVP and PVP/PLA electrospun nanofibers with/without curcumin. The authors used a drum collector (2000 rpm) for all types of fibers. Curcumin encapsulation into the polymer matrix leads to the increase of drug solubility into aqueous solutions. The effect observed could be explained by the complex formation between hydrophobic curcumin and hydrophilic PVP. Moreover, the polymer capsule allows the protection of curcumin from the destruction under UV-irradiation, which is necessary in the sterilization processes. The nanofibers obtained have good antibacterial effectiveness against the fungus *Candida albicans* and the Gram-positive bacteria *Staphylococcus aureus*. *In vitro* tumour cell viability assay was performed on HeLa and Graffi cancer cells and the cytotoxic effect of curcumin-loaded PVP nanofibers was confirmed. Moreover, it was shown that PVP nanofibers have good biocompatibility in contact with murine peritoneal macrophages and spleen lymphocytes for 72 h.

Yubo Liu *et al.* successfully obtained curcumin-loaded core-shell nanofibers based on PVP as the key polymer matrix



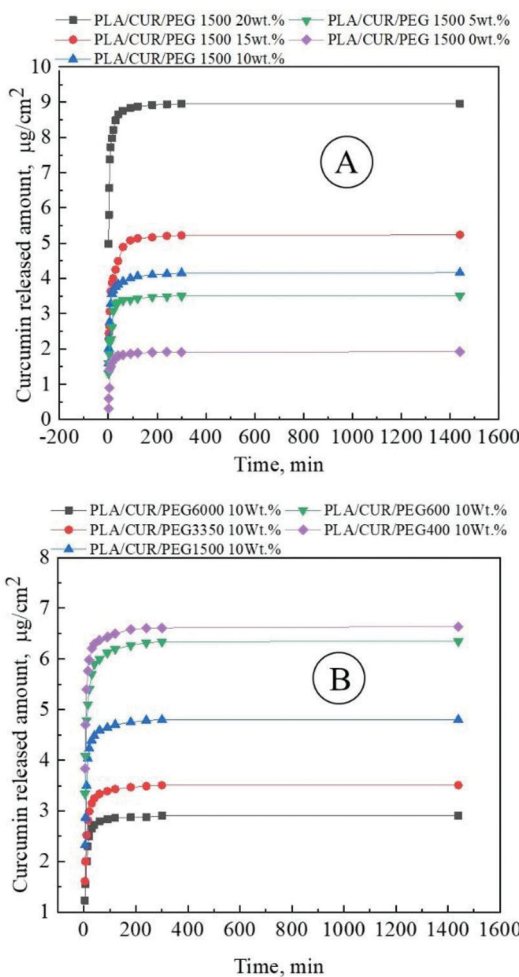


**Fig. 5** Curcumin release profile from curcumin-loaded PLA/PEG membranes electrospun from the polymer solutions: (A) 10 wt% PLA and various concentrations of PEG (from 0.0 to 20.0 wt% at a pitch of 5.0 wt% with respect to PLA); (B) 10 wt% PLA and 10 wt% PEG (related to PLA) with different molecular weights. Reproduced from ref. 48, with permission from Elsevier, 2022.

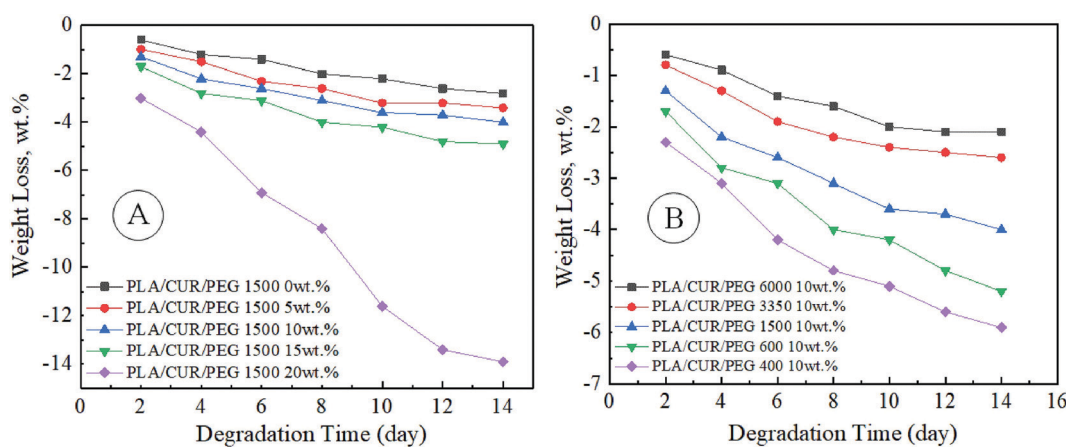


**Fig. 6** Weight loss of curcumin-loaded PLA/PEG nanofibers contained: (A) 10 wt% PLA and various concentration of PEG (from 0.0 to 20.0 wt% at a pitch of 5.0 wt% with respect to PLA); (B) 10 wt% PLA and 10 wt% PEG (related to PLA) with different molecular weights. Reproduced from ref. 48, with permission from Elsevier, 2022.

by the co-axial electrospinning technique.<sup>56,57</sup> The hydrophobic poly(3-hydroxybutyric acid-*co*-3-hydroxyvaleric acid) (PHBV) was used as an additional layer to regulate the hydrophilicity of the fibers obtained and limit the dissolution rate of curcumin.

The authors demonstrated that combination of the PVP and PHBV, as well as the core-shell structure of nanofibers obtained results in a unique drug delivery container with less tailing phenomena of sustained curcumin release.<sup>57</sup>

Hydrophilicity reduction of PHBV-coated fibers in comparison with native PVP-fibers (from  $31.42^\circ \pm 3.07^\circ$  to  $15.31^\circ \pm 2.79^\circ$ ) was demonstrated. PVP-fibers have rapid release rate with burst character (4 h to complete curcumin release). By contrast, core-shell fibers have dosing and constant-rate drug release profiles for 24 h.<sup>56</sup>

Interestingly, an energy saving electrospinning process of PVP-fibers with hydrophobic drugs is also available. Thus, Shixiong Kang *et al.*<sup>58</sup> used a concentric spinning nozzle with a Teflon-core rod, resulting in double reduction of energy consumption in comparison with the traditional method. Because the authors used ketoprofen as a model drug, detailed technological parameters were omitted here.

The abovementioned study highlights the importance of the spinning solution parameters, such as viscosity, for providing smooth and linear morphology of nanofibers.

PVP nanofibers due to the hydrophilic character of the basis polymer may be used in the applications with the rapid release of hydrophobic drugs, such as curcumin. The encapsulation of photosensitive natural biologically active agents allows them to maintain their properties and activity during photochemical degradation or sterilization procedures.

The information about the solution recipes and technological electrospinning parameters is listed in Table 4.

### 3.5 Polyvinyl alcohol

Polyvinyl alcohol (PVA) as a hydrophilic semi-crystalline synthetic polymer has high level of biocompatibility, biodegradability, and non-toxicity, that allows the use of PVA and its

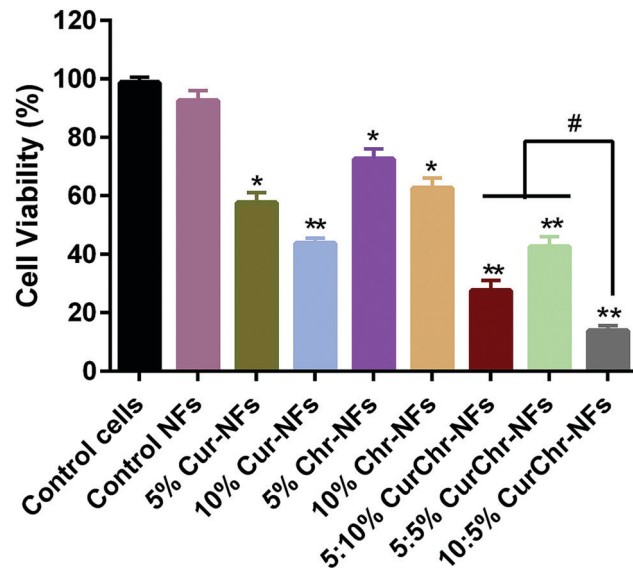


Fig. 7 *In vitro* cytotoxicity of the drug-loaded membranes against the T47D breast cancer cells after 3 days of the incubation. NFs – nanofibers, Cur – curcumin, and Chr – chrysanthemum. Reproduced from ref. 49, with permission from Elsevier, 2022.

composites as advanced food packaging, scaffolds for artificial tissue engineering, targeted delivery systems, *etc.*<sup>59</sup>

Xiao-Zhu Sun *et al.*<sup>60</sup> described nanofibers based on PVA with curcumin. The authors also investigated its complex with cyclodextrin which is well-characterized.<sup>61,62</sup> The detailed investigation confirmed the crystalline form of curcumin into PVA nanofibers. By contrast, the curcumin–cyclodextrin complex was better dispersed (loaded) in the polymer matrix. The nanofiber diameter increases with curcumin content decrease, but nanofibers with a curcumin–cyclodextrin complex have a tendency to diameter reduction with the increase of curcumin content. Curcumin/curcumin–cyclodextrin complex release profile has burst character for 320 min.

The next study<sup>63</sup> demonstrates the possibility of controlled release of curcumin by the crosslinking of PVA nanofibers.

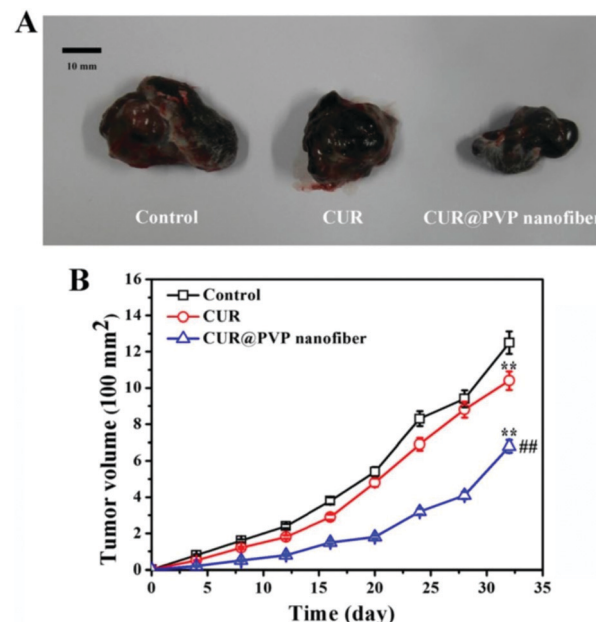


Fig. 8 (A) Photo of the tumours exposed to various medications at day 32; (B) the time dependent behaviour of tumour volume. Reproduced from ref. 53, with permission from Springer Nature, 2022.

The crosslinking was performed by heat treatment and UV-irradiation. Interestingly, the first one increased the nanofiber diameter, while the second one did not cause notable morphology change.

The curcumin release could be characterized as controlled (up to 20% for nanofibers after heat cross-linking and up to 9% after UV treatment in comparison with the fibers without cross-linking). Due to the cross-linking technique the swelling ratio of nanofibers was limited by 300%. Antibacterial activity against *Staphylococcus aureus* and *Escherichia coli* was confirmed: bacteria were totally dead within 6 h.

Mrunalini K. Gaydhane *et al.*<sup>64</sup> prepared multilayer PVA/cellulose acetate nanofibrous scaffolds. The authors also loaded into the polymer matrix raw honey. Nanofibers

Table 3 Solution recipes and technological parameters of electrospinning from the solutions based on poly(lactic) acid

Polymer base ( $M_w$ , kDa)	$C_{PB}$ , w/v%	Solvent(s), w/w or v/v	$C_{cur}$ , % w/w	FR, mL h <sup>-1</sup>	$U$ , kV	$H$ , mm	$D_{fib}$ , nm	Ref.
PLA (300.0)	4.2	MC/DMF 6.5 : 3.5 v/v	2.0 mg mL <sup>-1</sup>	1.2	20.0	150	3600 ± 1000	43
PLGA (50.0–75.0)	26.8	Acetonitrile	8.3 mg mL <sup>-1</sup>	0.9	13.0	150	123.6 ± 26.8	43
PDLA	15.0	—	0.0	0.5	15.0	125	200–250	44
HPG (Mn 15.0)	20.0	—	10.0	—	—	—	200–500	—
PLA (Mn 146.0)	10.0	CHCl <sub>3</sub> /acetone 2 : 1 v/v	0; 1; 3; 5; 7; 9; 11	0.5	18.0	120	1500 ± 900	45
PLA (75.0–120.0)	20.0	DMF/DCM	—	—	—	—	—	46
Chitosan	8.0	DMF/DW	—	—	—	—	—	—
PLLA (200.0)	10.0	DCM/DMF 7 : 3 v/v	0.0 0.2 0.5 1.0	n.r. — — —	24.0 — — —	150 — — —	386 ± 121 333 ± 124 351 ± 97 380 ± 113	47
PLA (Mn 146.0)	10.0	CHCl <sub>3</sub> /acetone 2 : 1 v/v	10.0	0.5	20.0	150	400–750	48
PEG (Mn 0.4–6.0)	0.0–20.0	—	—	—	—	—	—	—
PLGA/PEG copolymers (7.865)	10.0	DCM/methanol 4 : 1 v/v	5.0	2.0	22.0–25.0	200	400–500	49
Total			10.0					

$D_{fib}$  – average fiber diameter; DW – deionized water; HPG – hyperbranched polyglycerol; MC – methylene chloride; PDLA – poly DL lactic acid; PLA – poly(lactic) acid; PLGA – poly(lactic-*co*-glycolic acid); PLLA – poly(l-*l*-lactic acid);  $U$  – applied high voltage level.

Table 4 Solution recipes and technological parameters of electrospinning from the solutions based on polyvinylpyrrolidone

Polymer base ( $M_w$ , kDa)	$C_{PB}$ , w/v%	Solvent(s), w/w or v/v	$C_{cur}$ , % w/w	FR, mL h <sup>-1</sup>	$U$ , kV	$H$ , mm	$D_{fib}$ , nm	Ref.
PVP F90	5.0; 7.0; 10.0	EtOH/acetone 1:1 v/v	0.5; 0.7; 1.0	n.r.	4.9	n.r.	540–660	52
PVP F90	5.0; 7.0; 10.0	EtOH/acetone 1:1 v/v	0.5; 0.7; 1.0	n.r.	7.0	n.r.	350–400	52
Polysorbate 20								
PVP K90 (1300.0)	10.0	Acetic ether	0.0 10.0; 15.0; 20.0	2.0	15.0	150	888 ± 134 485 ± 123	53
PVP (1300.0)	10.0	EtOH/acetonitrile	5.0 10.0 15.0	2.0	12.0	150	n.r. 600 ± 50 n.r.	54
PVP (360.0)	~6.0	EtOH	0.0 10.0 15.0 20.0 25.0	3.0	25.0	100	502 ± 13 560 ± 126 692 ± 125 764 ± 164 1073 ± 177	55
PVP (360.0)	~4.8	DCM/DMSO	0.0	3.0	29.0	200	939 ± 184	55
PLA (165.85)	~4.8	2.5:1 v/v	15.0				1064 ± 191	
PVP K90 (130.0)	7.0	Ethanol	2.0	0.9	7.0	130	1230 ± 330	56
PHBV (natural origin, PHV content = 8 mol)	9.0	HFIP		1.4			1390 ± 270	
PVP K90 (130.0)	8.0	Ethanol	0.0	~1.04	7–8	160	930 ± 140	57
PHBV	10.0	HFIP	1.0	~1.56	7–8	160	830 ± 50	57
PVP K90 (130.0)	8.0	Ethanol	0.8	~1.04	7–8	160	1880 ± 280	57
PHBV	10.0	HFIP		~1.56				

$D_{fib}$  – average fiber diameter; DMSO – dimethyl sulfoxide; EtOH – ethanol; MC – methylene chloride; PLA – poly(lactic) acid; HFIP – hexafluoroisopropanol; PHBV – poly(3-hydroxybutyric acid-*co*-3-hydroxyvaleric acid).

Table 5 Solution recipes and technological parameters of electrospinning from the solutions based on polyvinyl alcohol

Polymer base ( $M_w$ , kDa)	$C_{PB}$ , w/v%	Solvent(s), w/w or v/v	$C_{cur}$ , % w/w	FR, mL h <sup>-1</sup>	$U$ , kV	$H$ , mm	$D_{fib}$ , nm	Ref.
PVA 1788	10.0	DW	5.0; 10.0; 15.0; 20.0	0.5	15.0	200	250–350	60
PVA (115.0)	10.0	20% acetic acid	0.0 1.0 2.0 5.0	1.0	15.0	100	223 ± 62 138 ± 53 129 ± 47 113 ± 31	63
PVA ( $n = 2000$ )	6.0	DW	1.0	0.75	17.0	100	~262.2	64

demonstrated effectiveness against *Escherichia coli* and high antioxidant activity. Moreover, nanofibers have shown to be suitable for the controlled wound healing vapor transmission rate and good absorbance capacity. In summary, the above-mentioned studies demonstrate the possibility for the controllable curcumin release from nanofibers which could become widely used in various biomedical applications.

The summarized information is listed below (Table 5).

### 3.6 Copolymers of acrylic (methacrylic) acid

Acrylic (methacrylic) polymers belong to attractive groups of biocompatible polymers for the targeted drug delivery systems due to the possibility to respond to various external influences such as pH, temperature, ions, electrical field, *etc.*, leading to structural changes and controllable drug release.<sup>65</sup>

A recent study<sup>66</sup> describes an electrospun nanofibrous scaffold based on the copolymer of acrylic and methacrylic acid esters Eudragit RS100 ( $C_{19}H_{34}ClNO_6$ ). Interestingly, the authors used needless electrospinning equipment with an intermediate rotary disc partially immersed into a solution bath. As a result, the smooth, bead-free, and uniform nanofibers were obtained and characterized. Incorporation of curcumin into the

polymer matrix and antibacterial activity of nanofibers against *Staphylococcus aureus* were demonstrated.

The next research article<sup>67</sup> demonstrates curcumin-loaded nanofibers based on the anionic copolymer of methacrylic acid and methyl methacrylate Eudragit L100. Fluorescence and antibacterial analyses were performed. The results confirmed the high curcumin-loading capacity of Eudragit L100 (250 mg mL<sup>-1</sup> in ethanol solution) and maintaining of the photochemical and photophysical characteristics of curcumin, and its significant antibacterial activity against *Staphylococcus aureus*. Fluorescence emission of nanofibers based on Eudragit L100 with curcumin at 360 nm is demonstrated in Fig. 9.

The summarized content and electrospinning parameters are listed in Table 6.

### 3.7 Polysaccharides

Polysaccharides are biocompatible, biodegradable, and non-toxic biopolymers having ultralow immunogenicity which could be used in biomedicine and biotechnology for diagnostic and drug (cell, gene, *etc.*) delivery systems, wound healing, various medical devices, theranostics, *etc.*<sup>68</sup>



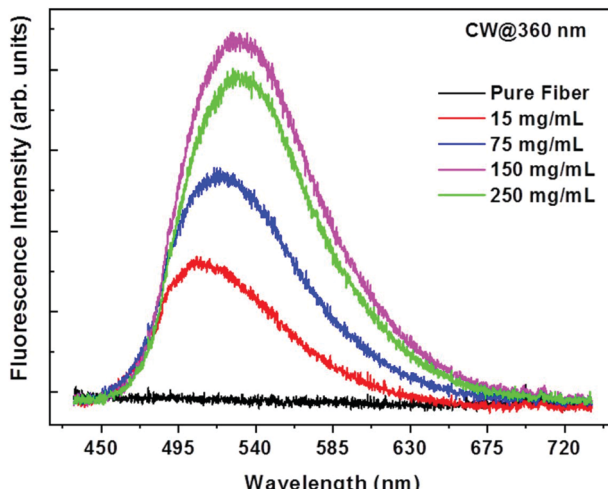


Fig. 9 Fluorescence emission of curcumin-loaded nanofibers based on Eudragit L100 at 360 nm with various curcumin concentrations in the spinning solution. Reproduced from ref. 67, with permission from Springer Nature, 2022.

Cellulose acetate (CA) is one of the most usable derivatives of cellulose which is the structural component of plant cell membrane and tissues. CA could be used as a raw natural material in various industrial applications, for instance, food industry, fiber technology, wood processing industry, medicine, drug delivery systems, *etc.* High porosity of materials based on cellulose allows the use of CA in biomedical and bioengineering applications, for filtration systems, food and goods packaging, building industry, *etc.*<sup>69</sup>

Cellulose acetate bead-free nanofibrous scaffolds with curcumin were successfully prepared and characterized.<sup>70</sup> The incorporation of curcumin into the CA nanofibers did not have a significant effect on the nanofiber morphology: blank CA nanofibers have an average diameter equal to 300 nm, and curcumin-loaded ones were slightly thicker (314–340 nm). In comparison with curcumin-loaded CA films, curcumin-loaded CA nanofibers have 90–95% releasing capacity. The original antioxidant activity of curcumin incorporated into CA nanofibers was maintained. The absence of cytotoxicity of curcumin-loaded CA nanofibers against normal human skin fibroblasts was confirmed.

As mentioned above, Mrunalini K. Gaydhane *et al.*<sup>64</sup> demonstrated a multilayer PVA/cellulose acetate/PVA nanofibrous material (Fig. 10), which has potential use as the advanced wound healing dressing with not only therapeutic effect belonging to natural components (curcumin and honey), but also with exudate absorption and controlled vapour permeability.

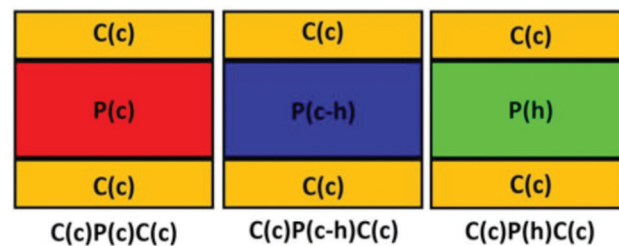


Fig. 10 Multilayer scaffold, where P – PVA, C – cellulose acetate, h – honey, and c – curcumin. Reproduced from ref. 64, with permission from Springer Nature, 2022.

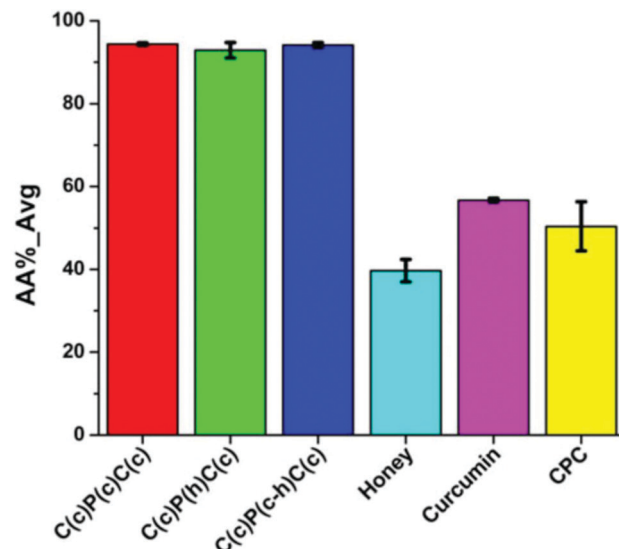


Fig. 11 Antioxidant activity of multilayer scaffold and native substances, where P – PVA, C – cellulose acetate, h – honey, and c – curcumin. Reproduced from ref. 64, with permission from Springer Nature, 2022.

Antioxidant activity of the multilayer nanofibrous material in comparison with natural biologically active agents is demonstrated in Fig. 11.

Hydroxypropyl methylcellulose (hypromellose, HPMC) as a most applied polymer for drug delivery<sup>71</sup> could be also used as a basis polymer for nanofiber production. Thus, Gamze Rüzgar *et al.*<sup>72</sup> developed curcumin-loaded nanofibers based on HPMC and PEO. The authors demonstrated that the initial crystal structure of curcumin did not become amorphic under the high-voltage electrospinning technique.

Drug loading was equal to 138 mg per square centimeter of HPMC/PEO nanofiber. Solubility of encapsulated curcumin in deionized water and acid buffer (pH = 1.2) was significantly

Table 6 Solution content and technological parameters of electrospinning from the solutions based on copolymers of acrylic acid

Polymer base ( $M_w$ , kDa)	$C_{PB}$ , w/v%	Solvent(s), w/w or v/v	$C_{cur}$ , % w/w	$FR$ , mL h <sup>-1</sup>	$U$ , kV	$H$ , mm	$D_{fib}$ , nm	Ref.
Eudragit RS100	8.0	EtOH/DMF 1:1 v/v	0.0; 1.0; 5.0; 9.0	—	35.0	120	n.r.	66
Eudragit L100	18.75	EtOH	0.0–250.0 mg mL <sup>-1</sup>	1.0	15.0	150	—	67

$D_{fib}$  – average fiber diameter; DMF – dimethylformamide; EtOH – ethanol.



higher than that of native curcumin which is practically insoluble (7.7 mg mL<sup>-1</sup> in deionized water and 1.6 mg mL<sup>-1</sup> in acid buffer respectively). In summary, the authors declared the possibility of such systems for oral drug systems of poorly soluble biologically active agents.

Chitosan is another member of the polysaccharide family, which could be obtained by enzymatic or chemical deacetylation of chitin. Due to the unique biochemical properties and ability to form nanofibers,<sup>73</sup> films,<sup>74</sup> hydrogels,<sup>75</sup> etc., chitosan attracts attention and could be used for challenging biomedical applications.<sup>76</sup>

Bhaarathi Dhurai with co-authors<sup>77</sup> obtained the curcumin-loaded chitosan/PLA nanofibers and analyzed their healing efficiency. The nanofibers demonstrated good antioxidant activity, which has an increasing tendency during the experiment. The curcumin release rate was maximal between 2 and 6 h. The drug-loaded chitosan/PLA nanofibers had no toxicity against the normal fibroblast cell line L-929. *In vivo* assay demonstrates the improved wound healing.

The next study<sup>78</sup> describes chitosan/PVA nanofibers with various molecular weights of chitosan. Interestingly, the authors used an unusual technique for the loading of curcumin into nanofibers: the preliminary electrospun nanofibers were submerged in curcumin/ethanol solution (5 wt%) for 24 h. The significant effect of chitosan molecular weight on nanofiber morphology was confirmed. Nanofibers based on 150 kDa chitosan have better absorption and release profile than nanofibers based on 200 kDa curcumin. The curcumin release rate was stable and prolonged for 148 h.

Adele Faralli *et al.*<sup>79</sup> developed curcumin-loaded nanofibers based on chitosan and xanthan gum. The authors

demonstrated that without the addition of xanthan the electrospinning process was not possible. Also, the curcumin addition led to the significant increase of nanofiber diameter. The results of cell viability assay against Caco-2 cells and transepithelial permeability across the monolayer cell barrier confirmed the possibility of the use of chitosan/xanthan nanofibers as oral drug systems for water-insoluble medications like curcumin.

Alginate is another polysaccharide that could be used as the polymer matrix of electrospun nanofibers. Thus, Javier Gutierrez-Gonzalez<sup>80</sup> reported cross-linked curcumin-loaded alginate/PEO nanofibers. The authors prepared two individual solutions of sodium alginate and PEO with further blending in a ratio of 29:9.5 (g alginate/g PEO). Such materials could be used in food packaging and absorption of pollution agents in wastewater.

Hyaluronic acid is a versatile biopolymer which is widely used for various applications, *e.g.* wound healing, artificial skin, infra-articular substitute of synovia, drug delivery systems, eye drops, gene therapy, cosmetics, etc.<sup>81</sup>

Hyaluronic acid nanofibers with curcumin were successfully obtained and characterized.<sup>82</sup> In the next study, usnic acid was loaded into a polymer matrix together with the curcumin.<sup>83</sup> The improvement of the electrospinning process was observed. Note that the additional polymers such as PEO or PVA were not used.

The summarized information is listed below (Table 7).

### 3.8 Proteins

The proteins are known as biodegradable, biocompatible, non-toxic biopolymers, for example, gelatin, silk fibroin, amaranth protein, zein from corn, etc., extracted from the tissues of living

Table 7 Solution recipes and technological parameters of electrospinning from the solutions based on polysaccharides

Polymer base ( $M_w$ , kDa)	$C_{PB}$ , w/v%	Solvent(s), w/w or v/v	$C_{cur}$ , % w/w	FR, mL h <sup>-1</sup>	$U$ , kV	$H$ , mm	$D_{fib}$ , nm	Ref.
CA (30.0)	17.0	Acetone/DMA 2:1 v/v	0.0	1.0	17.5	150	$301 \pm 64$	70
			5.0				$340 \pm 98$	
			10.0				$338 \pm 85$	
			15.0				$334 \pm 49$	
			20.0				$314 \pm 60$	
CA (29.0)	16.0	Acetone/DMA (2:1 v/v)	1.0	0.6	12.0	120	$\sim 329.5$	64
HPMC K100M	3.0	Methanol/DW 7:3 v/v	1.0 mg mL <sup>-1</sup>	0.6	14.0	210	$138 \pm 39$	72
PEO (600.0)	3.0							
Chitosan/PLA	5.5	TFA/DCM (8:2 v/v)	11.0	0.05	20.0	160	$\sim 66$	77
Chitosan	Diff.	Acetic acid (2%)	—	0.5	15.0	100	$\sim 200$	78
PVA (146.0–186.0)								
CTS/PVA ( $\leq 1/3$ )								
Chitosan (28.0)	3.0	Formic acid	0.0	0.01	25.0	100	$750 \pm 250$	79
Xanthan (2000.0)	0.75		2.0				$900 \pm 440$	
Alginate (40.0)	8.0	DW	10.0	0.3–1.0	15.0–23.0	150	212–250	80
PEO (1.0)	4.0		20.0					
			30.0					
			40.0					
Hyaluronic acid (1300.0)	1.9	DMSO/DW 1:1 v/v	1:1 – 1:25 (molecular ratio HA/Cur)	1.5–3.0	22.0	150	194–799	82
Hyaluronic acid (1300.0)	1.9	DMSO/DW 1:1 v/v	1:2 – 1:25 (molecular ratio HA/Cur)	2.0	22.0	150	146–630 153–1045	83
					28.0		130–803	

CA – cellulose acetate; CTS – chitosan;  $D_{fib}$  – average fiber diameter; DMA – *N,N*-dimethylacetamide; DMSO – dimethyl sulfoxide; HPMC – hydroxypropyl methylcellulose; TFA – trifluoroacetic acid.



organisms or from plant raw materials. The limitation for use of such polymers as the basis for electrospun nanofibers is related to the limited solubility in organic solvents, susceptibility to environmental conditions and treatments, and high pricing of the extraction and purification.<sup>84</sup> Collagen and gelatin are the key polymers used for obtaining electrospun nanofibers based on proteins. Collagen is the general component of the extracellular matrix (ECM) of living organisms. It has low solubility in water and for this reason the electrospinning of collagen-based nanofibers is hindered. In order to overcome this problem, the modifying polymers such as PEO or PCL are added to the spinning solution of collagen, similar to hyaluronic acid spinning solutions.<sup>85</sup> Interestingly, collagen–chitosan mixtures allow for obtaining systems having good spinnability due to polyion interactions between the two polymers.

Moreover, hexafluoro-2-propanol and 2,2,2-trifluoroethanol can be used for collagen dissolution, leading to an improvement in solution electrospinnability, but also to the alteration of collagen structure.<sup>86</sup>

Thus, Mohammad Ali Ghavim *et al.*<sup>87</sup> obtained the bone regeneration membranes based on collagen with the addition of curcumin and aspirin-loaded PLGA nanoparticles. Membranes prepared demonstrated both the retention of surrounding soft tissue from bone defects, and high antibacterial effect with bone healing activity generated by curcumin. The key characteristics of the membrane obtained are shown in Table 8.

The next study<sup>88</sup> demonstrates thin, porous, and lightweight curcumin-loaded gelatin nanofibers for potential wound healing and other applications. The authors analyzed the effect of various technological factors on electrospinning stability and fiber morphology in detail.

Ali Alehosseini *et al.*<sup>89</sup> encapsulated curcumin into both nanofibers based on gelatin and zein protein for packaging application. The latter is a biocompatible and biodegradable biopolymer, consisting of corn protein mixture and included equal to 45–50% of total corn proteins, and approximately 70% of endosperm proteins.<sup>90</sup> Additionally, the authors incorporated into a polymer matrix a green tea extract to analyze its effect on the stability, protective efficacy, and drug release profiles of curcumin-loaded nanofibers. The study showed that gelatin-based nanofibers have promising release in contact with fatty products; by contrast, zein-based nanofibers are more convenient for the packaging of aqueous products.

Narges Fereydouni *et al.*<sup>91</sup> developed nano-curcumin-loaded nanofibers based on native zein corn protein. Curcumin-loaded nanofibers exhibited a significant increase in proliferation of the mouse fibroblast cell line L929 and human dermal fibroblast (HDF) cell line. However, the antibacterial assay did not show any antibacterial impact of nanofibers against *Escherichia coli*, *Staphylococcus aureus*, and *Pseudomonas aeruginosa* due to low amount of nano-curcumin in nanofibers.

**Table 8** The key characteristics of the membrane obtained. Reproduced from ref. 87, with permission from Springer Nature, 2022

Main finding of tests	Collagen nanofibers (CNFs) including PANPs (PACNFs)	Curcumin/collagen nanofibers (CCNFs)
The asymmetric membrane		
Physical state	White sheet (thickness of 0.4 mm)	Yellow sheet (thickness of 0.4 mm)
The mean particle size and the surface charge	98.52 nm (PDI of 0.49)	84.06 nm (PDI of 0.39)
SEM results for morphology	With a negative surface charge of $-32.20\text{ mV}$ Nanofibers with a network structure and without the presence of beads	With a negative surface charge of $-37.74\text{ mV}$ Nanofibers with a network structure and without the presence of beads
<i>In vitro</i> cellular examinations	Without any toxic effect on DPSCs Increase in the proliferation of DPSCs ( $p < 0.05$ ) Increase in ALP activity ( $p < 0.05$ ) Increase in RNA expression of Runx-2, and OCN as osteogenic genes ( $p < 0.05$ ) Increase in protein expression of Runx-2, and OCN as osteogenic genes ( $p < 0.05$ ) Not showed any antimicrobial effects	Without any toxic effect on DPSCs Increase in the proliferation of DPSCs ( $p < 0.05$ ) Increase in ALP activity ( $p < 0.05$ ) Increase in RNA expression of Runx-2, and OCN as osteogenic genes ( $p < 0.05$ ) Increase in protein expression of Runx-2, and OCN as osteogenic genes ( $p < 0.05$ ) It showed antibacterial effects against <i>S. aureus</i> , <i>E. faecalis</i> and <i>E. coli</i> The membrane was more effective against <i>S. aureus</i> followed by <i>E. faecalis</i> and <i>E. coli</i>
Microbial test		
<i>In vivo</i> findings	The asymmetric membrane completely occupied after just 28 days, while the commercial membrane area remains empty. No significant inflammatory was detected in the pathology specimens, and the membranes were completely degraded. The results of the microscopic examination showed that new bone formation can be seen in the prepared membrane area. The newly created bone was detected in the test membrane in HE staining images, suggesting that the PACNFs layer of the membrane is osteoinductive and that the CCNFs layer not only can act as a physical barrier for the GBR technique, but also it also has osteoconductive effects (according to cellular results) that improves the PACNFs layer's action.	

ALP – alkaline phosphatase; CCNFs – curcumin/collagen nanofibers; CNFs – collagen nanofibers; DPSCs – dental pulp stem cells; HE – hematoxylin–eosin; GBR – guided bone regeneration; OCN – late marker of osteogenesis; PACNFs – collagen nanofibers including PLGA-aspirin nanoparticles; PANPs – pLGA-aspirin nanoparticles; PDI – polydispersity index; RNA – ribonucleic acid; Runx-2 – runt-related transcription factor 2 (early marker of osteogenic differentiation).



Silk fibroin being an important natural protein could be obtained from spiders (*Nephila clavipes dragline*) and silkworms (*Bombyx mori*). Silk fibroin is widely used in medical and bioengineering applications, such as tissue engineering, due to its high biocompatibility, slow biodegradability, and good mechanical characteristics.<sup>92</sup> It was proved that silk fibroin electrospun matrices enhance the burn wound healing and could be a challenging candidate for the wound treatment.<sup>93</sup>

Trangaraju Elakkiya *et al.* obtained curcumin-loaded electrospun nanofibers based on *Bombyx mori* silk fibroin.<sup>94</sup> The glass transition temperature of silk fibroin nanofibers was equal to 168 °C and in the case of curcumin addition increased to 184 °C. The cumulative release of curcumin from nanofibers containing 0.5, 1 and 1.5 wt% of drug was equal to 82%, 84%, and 80%, respectively.

Interestingly, the transition of crystalline structure of native curcumin to an amorphous state of curcumin loaded into nanofibers was detected.

The next study demonstrates curcumin-loaded nanofibers based on silk fibroin/poly(L-lactic acid-co-e-caprolactone).<sup>95</sup> The nanofibers exhibit high antibacterial activity against *Staphylococcus aureus* even with low curcumin content: bacterial inhibition was equal to 98.3 ± 0.29%, 99.3 ± 0.13%, and 99.7 ± 0.85% for nanofibers loaded with 2.0, 4.0, and 6.0 curcumin content (%, w/w).

Huijun Li *et al.*<sup>96</sup> used the curcumin-loaded into regenerated silk fibroin nanospheres and doxorubicin hydrochloride with the subsequent blending with aqueous-based regenerated silk fibroin solutions to form the single and dual drug-loaded

nanofibers. Nanofibers showed dual drug release profiles and stable release behavior.

The summarized information about the solution recipes and technological parameters of electrospinning is listed in Table 9.

## 4. Conclusion and future perspectives

The polymer matrixes are quite suitable tools for the incorporation of widely used curcumin. Curcumin being separated from *Curcuma longa* has attracted attention due to its anti-inflammatory, antimicrobial, antioxidant, antiviral and anticarcinogenic properties. As a typical natural compound, curcumin is non stable and has low solubility in water, which restricts its application as a drug molecule.

This review covered all known polymer systems with curcumin. Such systems were categorized into eight types, depending on polymer nature: poly( $\epsilon$ -caprolactone) and polydioxanone, polyurethanes, poly(lactic) acid and its derivatives, polyvinylpyrrolidone, polyvinyl alcohol, copolymers of acrylic (methacrylic) acid, polysaccharides, and proteins.

Among them fibers based on polyvinyl alcohol demonstrate the possibility for the controllable curcumin release and may be used as drug delivery systems with prolonged action.

Despite the limitations for proteins such as the limited solubility in organic solvents, susceptibility to environmental conditions and treatments, and high pricing of the extraction and purification, the nanofibers with very promising future

Table 9 Solution recipes and technological parameters of electrospinning from the solutions based on proteins

Polymer base ( $M_w$ , kDa)	$C_{PB}$ , w/v%	Solvent(s), w/w or v/v	$C_{cur}$ , % w/w	FR, mL h <sup>-1</sup>	$U$ , kV	$H$ , mm	$D_{fib}$ , nm	Ref.
Collagen (bovine type)	10.0	2,2,2-Trifluoroethanol	0.0 0.05 1.0	1.5	20.0	100	84.06	87
Gelatin	1.5	FA (98.0%)		0.1	15.0	100	147 ± 34/ 274 ± 53	88
Gelatin	2.0 20.0	AA (20.0%)	1.2 0.16 (liposomal curcumin dispersion)	0.15 0.15–1.50	20.0 12.0	150 100	89 ± 2	89
Zein (22–24)	20.0	Ethanol (80.0%)	0.16	0.15–1.50	12.0	100	89 ± 10	89
Zein	25.0	AA glacial	0.0 5.0 10.0 15.0	2.50	25.0	150	430 ± 142 340 ± 104 270 ± 60 220 ± 53	91
Silk fibroin from <i>Bombyx mori</i> silk cocoons	2.0–11.0	TFA	0.0	0.5	26.0	140	30–150	94
Silk fibroin from <i>Bombyx mori</i> silk cocoons + P(LLA-CL)	Σ 8.0	HFIP	0.5–1.5 2.0 4.0 6.0	1.2	10.0	150	50–200 365 ± 144 293 ± 110 497 ± 118	95
Silk fibroin from <i>Bombyx mori</i> silk cocoons	20.0	Water	3.0 1.0 + 0.1 DOX 3.0 + 0.1 DOX 5.0 + 0.1 DOX	0.9	30.0	150	1224 ± 410 982 ± 310 987 ± 340 1297 ± 380	96

AA – acetic acid; DOX – doxorubicin;  $D_{fib}$  – average fiber diameter; FA – formic acid; HFIP – hexafluoroisopropanol; TFA – trifluoroacetic acid; P(LLA-CL) – poly(L-lactic acid-co-e-caprolactone).



Table 10 Summarized data

No.	Polymer system ( $M_w$ , kDa)	Effects	Release	Ref.
1	PCL (65.0)	<ul style="list-style-type: none"> <li>Antioxidant properties were confirmed by oxygen radical absorbance capacity (ORAC);</li> <li>The high level of cytocompatibility, cytoprotective effectiveness, anti-inflammatory activity of curcumin-loaded nanofibers;</li> <li>Ability to accelerate the healing process <i>in vivo</i> (diabetic mouse model).</li> </ul>	<ul style="list-style-type: none"> <li>Time delayed: approximately 35 µg and 20 µg curcumin by day 3 from curcumin-loaded fibers with 17% w/w and 3% w/w, respectively.</li> </ul>	21
2	PCEC (61.8)	<ul style="list-style-type: none"> <li>High effectiveness against the rat Glioma 9L cells;</li> <li>Activity against the Glioma 9L cells was observed over the whole period of cytotoxicity assay, while the potency of native curcumin was lost within 48 h.</li> </ul>	<ul style="list-style-type: none"> <li>By day 14 the maximum curcumin amount was equal to 54.8%, 73.5%, 88.5%, and 90.7% for PCEC fibers with 5, 10, 15, 20 wt% of curcumin, respectively.</li> </ul>	22
3	PCEC (62.0)	<ul style="list-style-type: none"> <li>High absorbing capacity of free radicals;</li> <li>Low cytotoxicity against the primary mouse dermal fibroblast cells culture;</li> <li>Accelerate of the wound healing process (full-thickness skin defects model).</li> </ul>	<ul style="list-style-type: none"> <li>Slow release rate: 52.7%, 66.4%, 78.5%, and 87.2% for the nanofibers with 5%, 10%, 15%, and 20% for curcumin, respectively.</li> </ul>	23
4	PCL (80.0)	<ul style="list-style-type: none"> <li>Favoured cellular growth, cell attachment, cell proliferation and could retain initial cell morphology for 15 days.</li> </ul>	<ul style="list-style-type: none"> <li>Without burst effect.</li> </ul>	24
5	PCL (80.0)	<ul style="list-style-type: none"> <li>High antibacterial activity against methicillin resistant <i>Staphylococcus aureus</i> (99.9%) and extended spectrum <math>\beta</math>-lactamase (85.14%);</li> </ul>		24
	GT	<ul style="list-style-type: none"> <li>Accelerate the wound repair process;</li> <li>The increase of collagen content during the treating of diabetic wounds;</li> <li>Blood glucose level decrease.</li> </ul>		
6	PCL (80.0)	<ul style="list-style-type: none"> <li>Prevent the formation of postsurgical adhesion in animal model for 50% compared to the control group.</li> </ul>	<ul style="list-style-type: none"> <li>30% after 30 days.</li> </ul>	26
7	PCL (70.0), CTS (100.0–300.0)		<ul style="list-style-type: none"> <li>Curcumin released within 100 h (nearly 80%), further release rate decreased and around 90% of curcumin was released after 650 h.</li> </ul>	27
8	PCL (80.0)		<ul style="list-style-type: none"> <li>Release ratio is slow and without any burst effect.</li> </ul>	28
9	PCL (80.0), PEO (100.0)	<ul style="list-style-type: none"> <li>High level of toxicity against MCF-7 breast cancer cells.</li> </ul>	<ul style="list-style-type: none"> <li>The maximizing of curcumin encapsulation efficiency and deceleration of curcumin release.</li> </ul>	29
10	PCL (80.0), PHB (1000.0)		<ul style="list-style-type: none"> <li>The reduction of burst release, resulting in the possibility of controllable curcumin release profile.</li> </ul>	30
11	PCL (80.0), silk fibroin		<ul style="list-style-type: none"> <li>Initial burst character within 3 h with further stable and slow release during 10 days.</li> </ul>	31
12	PCL (24.0)	<ul style="list-style-type: none"> <li>The formation of pathogenic biofilms belonged to the three bacteria strains: <i>Pseudomonas aeruginosa</i>, <i>Staphylococcus aureus</i> and <i>Escherichia coli</i></li> </ul>		32
13	PU2000, PU530	<ul style="list-style-type: none"> <li>Antibacterial effectiveness against <i>Escherichia coli</i> <i>in vitro</i> (up to 97% activity).</li> </ul>	<ul style="list-style-type: none"> <li>Burst release within 24 h, with further stable release over 450 h.</li> </ul>	38
14	PCL-based polyurethane (PU); Di-block PEG– PCL-based polyurethane (PCE)	<ul style="list-style-type: none"> <li>Antibacterial effect was equal to 93% and 100% against <i>Staphylococcus aureus</i> and <i>Escherichia coli</i>, respectively;</li> <li>Nontoxic effect was confirmed by metabolic activity of L929 mouse fibroblast cells.</li> </ul>	<ul style="list-style-type: none"> <li>Stable rate within 18 days.</li> </ul>	39
15	Taxoflex EG 85 A, Dextran (70.0)	<ul style="list-style-type: none"> <li>Synergistic antibacterial effectiveness against <i>Staphylococcus aureus</i>;</li> <li>Wound dressing with antibacterial properties.</li> </ul>	<ul style="list-style-type: none"> <li>pH-controlled release carriers.</li> </ul>	41
16	PDIA, HPG (Mn 15.0)	<ul style="list-style-type: none"> <li>High cytocompatibility with embryonic Swiss mouse fibroblast cells (3T3 line)</li> </ul>		44
17	PLA (Mn 146.0)			
18	PLA (75.0–120.0), chitosan	<ul style="list-style-type: none"> <li>Cytocompatibility of nanofibers with murine fibroblast L929</li> </ul>	<ul style="list-style-type: none"> <li>Burst release profile (60 min)</li> <li>Burst release in the first 24 hours (first phase) and controlled and slow character in the second (84 days) and third phases (the latter 7 days)</li> </ul>	45 46
19	PLLA (200.0)	<ul style="list-style-type: none"> <li>Antioxidant activity, non-toxicity of nanofibers to human adult dermal fibroblast, cell adhesion and proliferation</li> </ul>		47
20	PLA (Mn 146.0), PEG (Mn 0.4–6.0)	<ul style="list-style-type: none"> <li>Good cell attachment was confirmed by MG-63 cells adhesion assay</li> </ul>	<ul style="list-style-type: none"> <li>Curcumin release could be promoted as a result of PEG molecular weight decrease or PEG concentration increase</li> </ul>	48
21	PLGA/PEG copolymers (7.865)	<ul style="list-style-type: none"> <li>Inhibit T47D breast cancer cells</li> </ul>	<ul style="list-style-type: none"> <li>More prolonged drug release profile</li> </ul>	49



Table 10 (continued)

No.	Polymer system ( $M_w$ , kDa)	Effects	Release	Ref.
22	PVP F90, PVP F90, polysorbate 20		• The increase of release at the first stage. More than 50% of curcumin released regardless of spinning solution recipes	52
23	PVP K90 (1300.0)	• Dissolution profile, pharmacokinetics, bioavailability, and cytotoxicity ( <i>in vitro</i> and <i>in vivo</i> ) against murine melanoma cell line B16		53
24	PVP (360.0)	• Good antibacterial effectiveness against the fungus <i>Candida albicans</i> and the Gram-positive bacteria <i>Staphylococcus aureus</i> . • <i>In vitro</i> tumour cell viability assay was performed on HeLa and Graffi cancer cells.		55
25	PVA 1788		• Burst character	60
26	PVA (115.0)	• Antibacterial activity against <i>Staphylococcus aureus</i> and <i>Escherichia coli</i> was confirmed: bacteria totally dead within 6 h.	• Controlled (up to 20%) for nanofibers after heat cross-linking and up to 9% after UV treatment	63
27	PVA ( $n = 2000$ )	• Effectiveness against <i>Escherichia coli</i> ; • High antioxidant activity; • The controlled wound healing vapor transmission rate and good absorbance capacity.		64
28	Eudragit RS100	• Antibacterial activity against <i>Staphylococcus aureus</i>		66
29	Eudragit L100	• Significant antibacterial activity against <i>Staphylococcus aureus</i>		67
30	Chitosan/PLA	• Good antioxidant activity; • No toxicity against normal fibroblast cell line L-929; • <i>In vivo</i> assay demonstrates the improved wound healing.	• Release rate was maximal between 2 and 6 h	77
31	Chitosan PVA (146.0–186.0) CTS/PVA ( $\leq 1/3$ )		• Stable and prolonged during for 148 h	78

applications have been created. This has to be taken into account especially in the case of tissue engineering.

The results summarized in Table 10 illustrate that the introduction of curcumin into polymer fibers imparts antioxidant properties and most of those systems have antibacterial activity against *Staphylococcus aureus* and *Escherichia coli*.

Further perspectives have to be connected with pre-clinical studies of known systems, as well as with new fiber fabrication based on systems with the controlled release.

## Author contributions

Conceptualization, P. S. and S. M.; formal analysis, P. S. and S. M.; funding acquisition, M. U.; resources, P. S. and S. M.; supervision, S. M., R. O. and M. U.; visualization, P. S.; writing – original draft, P. S. and S. M.; writing – review & editing, P. S. and S. M. All authors have read and approved the manuscript.

## Conflicts of interest

There are no conflicts to declare.

## Acknowledgements

This work was supported by the Ministry of Science and Higher Education of the Russian Federation (agreement no. 075-15-2021-1349).

## References

- 1 N. Shavisi and Y. Shahbazi, *Food Packag. Shelf Life*, 2022, 32, 100827.
- 2 S. C. Gupta, S. Patchva and B. B. Aggarwal, *AAPS J.*, 2013, 15, 195–218.
- 3 B. B. Aggarwal and K. B. Harikumar, *Int. J. Biochem. Cell Biol.*, 2009, 41, 40–59.
- 4 Y. Panahi, M. S. Hosseini, N. Khalili, E. Naimi, L. E. Simental-Mendia, M. Majeed and A. Sahebkar, *Biomed. Pharmacother.*, 2016, 82, 578–582.
- 5 J. Trujillo, Y. I. Chirino, E. Molina-Jijón, A. C. Andérica-Romero, E. Tapia and J. Pedraza-Chaverri, *Redox Biol.*, 2013, 1, 448–456.
- 6 P. Anand, A. B. Kunnumakkara, R. A. Newman and B. B. Aggarwal, *Mol. Pharmaceutics*, 2007, 4, 807–818.
- 7 V. Kuptniratsaikul, P. Dajpratham, W. Taechaarpornkul, M. Buntragulpoontawee, P. Lukkanapichonchut, C. Chootip, J. Saengsuwan, K. Tantayakom and S. Laongpech, *Clin. Interventions Aging*, 2014, 9, 451–458.
- 8 F. Mazzolani and S. Togni, *Clin. Ophthalmol.*, 2013, 7, 939–945.
- 9 ClinicalTrials.gov Identifier: NCT03016039. Curcumin Supplementation for Gynecological Diseases – Full Text View. URL: <https://clinicaltrials.gov/ct2/show/NCT03016039?cond=curcumin&draw=2&rank=1>.
- 10 N. E. Elsadek, A. Nagah, T. M. Ibrahim, H. Chopra, G. A. Ghonaim, S. E. Emam, S. Cavalu and M. S. Attia, *Materials*, 2022, 15, 1934.



11 J. Li, Y. Liu and H. E. Abdelhakim, *Molecules*, 2022, **27**, 1803.

12 T. Ning, Y. Zhou, H. Xu, S. Guo, K. Wang and D.-G. Yu, *Membranes*, 2021, **11**, 802.

13 K. Zhou, M. Wang, Y. Zhou, M. Sun, Y. Xie and D.-G. Yu, *Adv. Compos. Hybrid Mater.*, 2022, **5**, DOI: [10.1007/s42114-021-00389-9](https://doi.org/10.1007/s42114-021-00389-9).

14 H. Xu, X. Xu, S. Li, W.-L. Song, D.-G. Yu and S. W. Annie Bligh, *Biomolecules*, 2021, **11**, 1330.

15 X. Liu, H. Xu, M. Zhang and D.-G. Yu, *Membranes*, 2021, **11**, 770.

16 W. Liu, J. Zhang and H. Liu, *Polymers*, 2019, **11**, 954.

17 D. G. Yu, M. Wang and R. Ge, *Wiley Interdiscip. Rev.: Nanomed. Nanobiotechnol.*, 2021, **2021**, e1772.

18 H. He, M. Wu, J. Zhu, Y. Yang, R. Ge and D.-G. Yu, *Adv. Fiber Mater.*, 2022, **4**, 305–317.

19 M. Zhang, W. Song, Y. Tang, X. Xu, Y. Huang and D. Yu, *Polymers*, 2022, **14**, 351.

20 V. R. Sinha, K. Bansal, R. Kaushik, R. Kumria and A. Trehan, *Int. J. Pharm.*, 2004, **278**(1), 1–23.

21 J. G. Merrell, S. W. McLaughlin, L. Tie, C. T. Laurencin, A. F. Chen and L. S. Nair, *Clin. Exp. Pharmacol. Physiol.*, 2009, **36**(12), 1149–1156.

22 G. Guo, S. Fu, L. Zhou, H. Liang, M. Fan, F. Luo, Z. Qian and Y. Wei, *Nanoscale*, 2011, **3**(9), 3825–3832.

23 S. Z. Fu, X. H. Meng, J. Fan, L. L. Yang, Q. L. Wen, S. J. Ye, S. Lin, B. Q. Wang, L. L. Chen, J. B. Wu, Y. Chen, J. M. Fan and Z. Li, *J. Biomed. Mater. Res., Part B*, 2014, **102**(3), 533–542.

24 M. Ranjbar-Mohammadi and S. H. Bahrami, *Int. J. Biol. Macromol.*, 2016, **84**, 448–456.

25 M. Ranjbar-Mohammadi, S. Rabbani, S. H. Bahrami, M. T. Joghataei and F. Moayer, *Mater. Sci. Eng., C*, 2016, **69**, 1183–1191.

26 S. Boroumand, S. Hosseini, M. Salehi and R. Faridi Majidi, *Nanomed. Res. J.*, 2017, **2**(1), 64–72.

27 M. Hoang, N. Doan and D. Huynh, *Vietnam J. Sci. Technol.*, 2018, **55**, 99–108.

28 R. Ramakrishnan, P. Ramakrishnan, B. Ranganathan, C. Tan, T. M. Sridhar and J. Gimbut, *Mater. Today: Proc.*, 2019, **19**(4), 1241–1246.

29 Y. Bülbül, M. Okur, F. Demirtaş Korkmaz and N. Dilsiz, *Appl. Clay Sci.*, 2020, **186**, 105430.

30 G. Gorrasi, R. Longo and G. Viscusi, *Polymers*, 2020, **12**(10), 2239.

31 B. Caglayan and G. Basal, *Dig. J. Nanomater. Biostructures*, 2020, **15**(4), 1165–1173.

32 D. A. Pompa-Monroy, P. G. Figueroa-Marchant, S. G. Dastager, M. N. Thorat, A. L. Iglesias, V. Miranda-Soto, G. L. Pérez-González and L. J. Villarreal-Gómez, *Materials*, 2020, **13**(23), 5556.

33 J. A. Martins, A. A. Lach, H. L. Morris, A. J. Carr and P.-A. Mouthuy, *J. Biomater. Appl.*, 2020, **34**(7), 902–916.

34 P. A. Mouthuy, S. M. Somogyi, A. Čipak Gašparović, L. Milković, A. J. Carr and N. Žarković, *Int. J. Nanomed.*, 2017, **12**, 3977–3991.

35 P. Alves, P. Ferreira and M. H. Gil, *Biomedical Polyurethane-Based Materials, Polyurethane: Properties, Structure and Applications*, Nova Publishers, New York, 2012, ISBN: 978-1-61942-453-1.

36 J. Akindoyo, M. Beg, S. Ghazali, M. Islam, N. Jeyaratnam and A. Yuvaraj, *RSC Adv.*, 2016, **6**, 114453–114482.

37 J. Joseph, R. M. Patel, A. Wenham and J. R. Smith, *Trans. IMF*, 2018, **96**(3), 121–129.

38 A. Shababdoust, M. Ehsani, P. Shokrollahi and M. Zandi, *Prog. Biomater.*, 2018, **7**, 23–33.

39 A. Shababdoust, M. Zandi, M. Ehsani, P. Shokrollahi and R. Foudazi, *Int. J. Pharm.*, 2020, **575**, 118947.

40 N. Horzum Polat and N. Arik Kinali, *Cumhur. Sci. J.*, 2019, **40**(1), 125–135.

41 P. Sagitha, C. R. Reshma, S. P. Sundaran, A. Binoy, N. Mishra and A. Sujith, *Int. J. Biol. Macromol.*, 2019, **126**, 717–730.

42 T. Casalini, F. Rossi, A. Castrovinci and G. Perale, *Front. Bioeng. Biotechnol.*, 2019, **7**, 259.

43 P. Luz, M. Silva and J. Hinestroza, *Int. J. Polym. Anal. Charact.*, 2013, **18**(7), 534–544.

44 G. Perumal, A. M. Nandkumar and M. Doble, *Front. Bioeng. Biotechnol. Conference Abstract: 10th World Biomaterials Congress*, 2016.

45 L. Moradkhannejhad, M. Abdouss, N. Nikfarjam, S. Mazinani and P. Sayar, *Fibers Polym.*, 2017, **18**, 2349–2360.

46 K. Matskou, V. Karagkiozaki, A. R. Tsiapla, V. Bakola, M. Pitou, E. Papadopoulou, S. Kassavetis, E. Pavlidou and S. Logothetidis, *Mater. Today: Proc.*, 2019, **19**(1), 117–125.

47 P. Pankongadisak, S. Sangklin, P. Chuysinuan, O. Suwantong and P. Supaphol, *J. Drug Delivery Sci. Technol.*, 2019, **53**, 101121.

48 L. Moradkhannejhad, M. Abdouss, N. Nikfarjam, M. H. Shahriari and V. Heidary, *J. Drug Delivery Sci. Technol.*, 2020, **56**(A), 101554.

49 S. Rasouli, M. Montazeri, S. Mashayekhi, S. Sadeghi-Soureh, M. Dadashpour, H. Mousazadeh, A. Nobakht, N. Zarghami and Y. Pilehvar-Soltanahmadi, *J. Drug Delivery Sci. Technol.*, 2020, **55**, 101402.

50 P. Franco and I. De Marco, *Polymers*, 2020, **12**, 1114.

51 H.-H. Utkarsh, M. Tariq, N. A. Syed, G. M. Rizvi and R. Pop-Iliev, *Adv. Polym. Technol.*, 2020, **2020**, 4090747.

52 A. Rahma, M. M. Munir, K. Khairurrijal and H. Rachmawati, *Adv. Mater. Res.*, 2015, **1112**, 429–432.

53 C. Wang, C. Ma, Z. Wu, H. Liang, P. Yan, J. Song, N. Ma and Q. Zhao, *Nanoscale Res. Lett.*, 2015, **10**, 439.

54 R. Rramaswamy, G. Mani and H. T. Jang, *J. Appl. Pharm. Sci.*, 2018, **8**(08), 26–31.

55 G. Yakub, A. Toncheva, V. Kussovski, R. A. Toshkova, A. Georgieva, E. B. Nikolova, N. Manolova and I. Rashkov, *Fibers Polym.*, 2020, **21**, 55–65.

56 Y. Liu, X. Chen, Y. Liu, Y. Gao and P. Liu, *Polymers*, 2022, **14**, 469.

57 Y. Liu, X. Chen, D. Yu, H. Liu, Y. Liu and P. Liu, *Mol. Pharmaceutics*, 2021, **18**(11), 4170–4178.

58 S. Kang, S. Hou, X. Chen, D.-G. Yu, L. Wang, X. Li and G. R. Williams, *Polymers*, 2020, **12**, 2421.

59 Y. Zhang, R. Remadevi, J. P. Hinestroza, X. Wang and M. Naebe, *Polymers*, 2020, **12**, 1190.

60 X. Z. Sun, G. R. Williams, X. X. Hou and L. M. Zhu, *Carbohydr. Polym.*, 2013, **94**(1), 147–153.



61 J. Chen, X. Qin, S. Zhong, S. Chen, W. Su and Y. Liu, *Molecules*, 2018, **23**(5), 1179.

62 M. Kasapoglu-Calik and M. Ozdemir, *J. Appl. Polym. Sci.*, 2019, **136**, 47554.

63 M. M. Mahmud, S. B. Zaman, A. Perveen, R. A. Jahan, M. F. Islam and M. T. Arafat, *J. Drug Delivery Sci. Technol.*, 2020, **55**, 101386.

64 M. Gaydhane, J. Kanuganti and C. Sharma, *J. Mater. Res.*, 2020, **35**(6), 600–609.

65 S. Vijay, O. P. Sati and D. K. Majumdar, *J. Mater. Sci.: Mater. Med.*, 2010, **21**, 2583–2592.

66 J. A. Awan, S. U. Rehman, M. Kashif Bangash, F. Hussain and J.-N. Jaubert, *Text. Res. J.*, 2020, **91**(13–14), 1478–1485.

67 M. C.-A. de Oliveira, F. A.-G. da Silva, M. M. da Costa, N. Rakov and H. P. de Oliveira, *Adv. Fiber Mater.*, 2020, **2**, 256–264.

68 M. Li, J. Ding, Y. Tao, B. Shi and J.-H. Chen, *Int. J. Polym. Sci.*, 2019, **2019**, 7841836.

69 U. G.-T. M. Sampath, Y. C. Ching, C. H. Chuah, J. J. Sabariah and P.-C. Lin, *Materials*, 2016, **9**, 991.

70 O. Suwantong, P. Opanasopit, U. Ruktanonchai and P. Supaphol, *Polymer*, 2007, **48**(26), 7546–7557.

71 E. Mašková, K. Kubová, B. T. Raimi-Abraham, D. Villasaliu, E. Vohlídalová, J. Turánek and J. Mašek, *J. Controlled Release*, 2020, **324**, 695–727.

72 R. Gamze, B. Mehmet, T. Serdar and A. Füsün, *FABAD J. Pharm. Sci.*, 2013, **38**(3), 143–149.

73 N. D. Al-Jbour, M. D. Beg, J. Gimbu and A. K.-M. M. Alam, *Curr. Drug Delivery*, 2019, **16**(4), 272–294.

74 J. I. Lozano-Navarro, N. P. Díaz-Zavala, C. Velasco-Santos, J. A. Melo-Banda, U. Páramo-García, F. Paraguay-Delgado, R. García-Alamilla, A. L. Martínez-Hernández and S. Zapién-Castillo, *Materials*, 2018, **11**, 120.

75 H. Liu, C. Wang, C. Li, Y. Qin, Z. Wang, F. Yang, Z. Li and J. Wang, *RSC Adv.*, 2018, **8**, 7533–7549.

76 D. Elieh-Ali-Komi and M. R. Hamblin, *Int. J. Adv. Res.*, 2016, **4**(3), 411–427.

77 B. Dhurai, N. Saraswathy, R. Maheswaran, P. Sethupathi, P. Vanitha, S. Vigneshwaran and V. Rameshbabu, *Front. Mater. Sci.*, 2013, **7**, 350–361, DOI: [10.1007/s11706-013-0222-8](https://doi.org/10.1007/s11706-013-0222-8).

78 D. V.-H. Thien, T. T.-B. Quyen, N. M. Tri, T. T.-K. Thoa and N. T.-N. Tham, *J. Sci. Technol.*, 2016, **54**(4B), 185–192.

79 A. Faralli, E. Shekarforoush, F. Ajalloueian, A. C. Mendes and I. S. Chronakis, *Carbohydr. Polym.*, 2019, **206**, 38–47.

80 J. Gutierrez-Gonzalez, E. Garcia-Cela, N. Magan and S. S. Rahatekar, *Mater. Lett.*, 2020, **270**, 127662, DOI: [10.1016/j.matlet.2020.127662](https://doi.org/10.1016/j.matlet.2020.127662).

81 K. Valachová and L. Šoltés, *Molecules*, 2021, **26**, 1195.

82 P. P. Snetkov, V. E. Sitnikova, M. V. Uspenskaya, S. N. Morozkina and R. O. Olekhovich, *Russ. Chem. Bull.*, 2020, **69**, 596–600.

83 P. Snetkov, S. Morozkina, R. Olekhovich, T. H.-N. Vu, M. Tyanutova and M. Uspenskaya, *Materials*, 2020, **13**, 3476.

84 Y. A. Ince and Ö. Tarhan, *Muğla J. Sci. Technol.*, 2020, **6**(2), 52–62.

85 P. Snetkov, S. Morozkina, M. Uspenskaya and R. Olekhovich, *Polymers*, 2019, **11**, 2036.

86 S. Wilk and A. Benko, *J. Funct. Biomater.*, 2021, **12**, 26.

87 M. A. Ghavimi, A. Bani Shahabadi, S. Jarolmasjed, M. Y. Memar, S. Maleki Dizaj and S. Sharifi, *Sci. Rep.*, 2020, **10**(1), 18200.

88 N. J. Kanu, E. Gupta, U. K. Vates and G. K. Singh, *Mater. Res. Express.*, 2020, **7**(3), 035022.

89 A. Alehosseini, L. Gómez-Mascaraque, M. Martinez-Sanz and A. López-Rubio, *Food Hydrocolloids*, 2019, **87**, 758–771.

90 A. Raza, U. Hayat, M. Bilal, H. Iqbal and J.-Y. Wang, *J. Drug Delivery Sci. Technol.*, 2020, **58**, 101818.

91 N. Fereydouni, J. Movaffagh, N. Amiri, S. Darroudi, A. Gholoobi, A. Goodarzi, A. Hashemzadeh and M. Darroudi, *Sci. Rep.*, 2021, **11**, 1902.

92 R. Obregón, J. Ramón-Azcón and S. Ahadian, Nanofiber composites in blood vessel tissue engineering, in *Nanofiber Composites for Biomedical Applications*, ed. M. Ramalingam, S. Ramakrishna, Woodhead Publishing, 2017, pp. 483–506, ISBN 9780081001738.

93 H. W. Ju, O. J. Lee, J. M. Lee, B. M. Moon, H. J. Park, Y. R. Park, M. C. Lee, S. H. Kim, J. R. Chao, C. S. Ki and C. H. Park, *Int. J. Biol. Macromol.*, 2016, **85**, 29–39.

94 T. Elakkiya, G. Malarvizhi, S. Rajiv and T. S. Natarajan, *Polym. Int.*, 2014, **63**, 100–105.

95 Y. Lian, J.-C. Zhan, K.-H. Zhang and X.-M. Mo, *Front. Mater. Sci.*, 2014, **8**(4), 354–362.

96 H. Li, J. Zhu, S. Chen, L. Jia and Y. Ma, *RSC Adv.*, 2017, **7**(89), 56550–56558.

